Power Electronic Systems Laboratory

ETH zürich

Part 4

1st Gen. 600 V GaN MBDSs in AC-AC CSCs and 3-Level T-Type VSCs

Jonas Huber, Neha Nain, Franz Vollmaier, Johann W. Kolar

Power Electronic Systems Laboratory
ETH Zürich

March 20, 2022

APEC 2★22

The Switch: 600 V, 140 mΩ GaN MBDS 1. Gen. Samples

- **BDS realization from unipolar devices: 4 x Single switch for same R_{on}!**

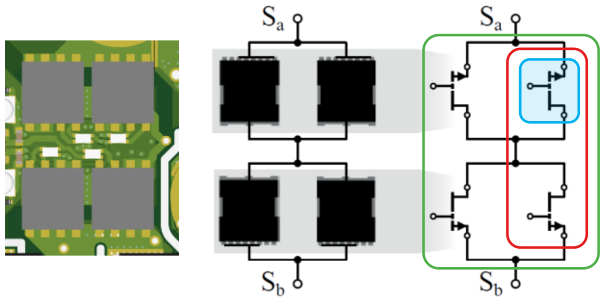

R_{on}

$R_{total} = 2R_{on}$

$R_{total} = R_{on}$

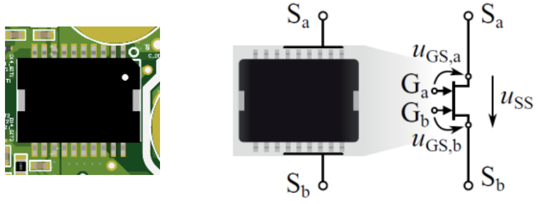

Package Image Source: https://www.infineon.com/cms/en/product/packages/PG-DSO/PG-DSO-20-85/

- ±600 V
- 140 mΩ
- PG-DSO-20-85 Package

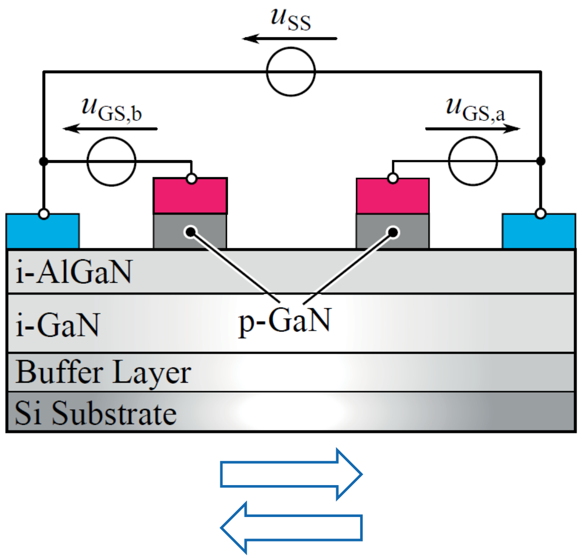

Same chip region used for blocking both voltage polarities: *True* MBDS!

- **GaN MBDS based on Infineon's 600 V CoolGaN™ technology**
  - Normally-off gate injection transistor (GIT) | Two gates (one per blocking direction) | Int. common-drain conf.

The Topologies

GaN/SiC 3-Level T-Type AC-DC PFC Rect. / DC-AC Inv.

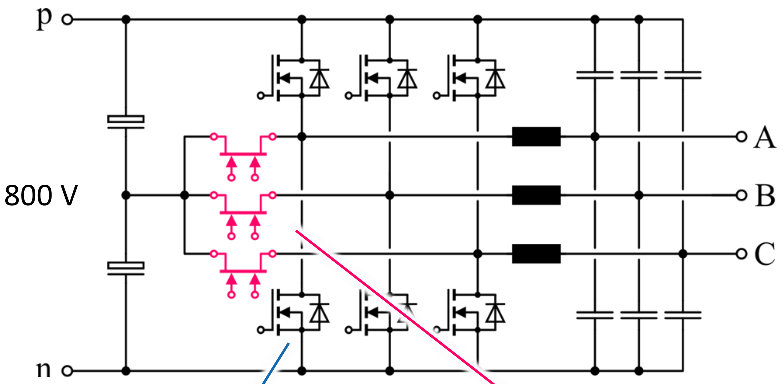

1200 V, 140 mΩ SiC

All-GaN AC-AC Current-Source Converter (CSC)

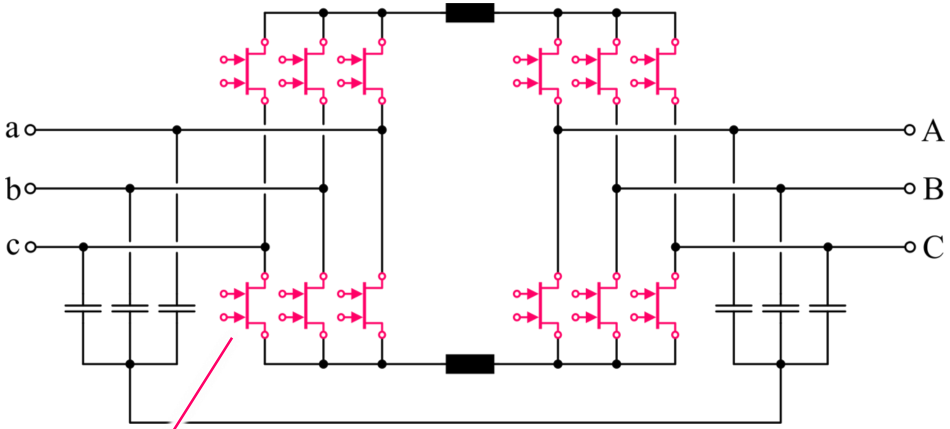

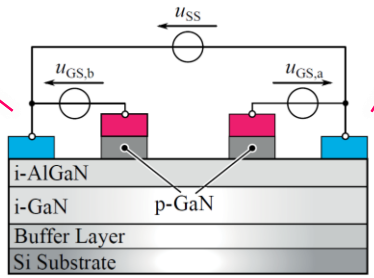

600 V, 140 mΩ
GaN M-BDS

GaN MBDS Gate Drive Considerations

GaN Gate Injection Transistor (GIT) Gate Behavior

Simplified MOSFET Gate Turn-On

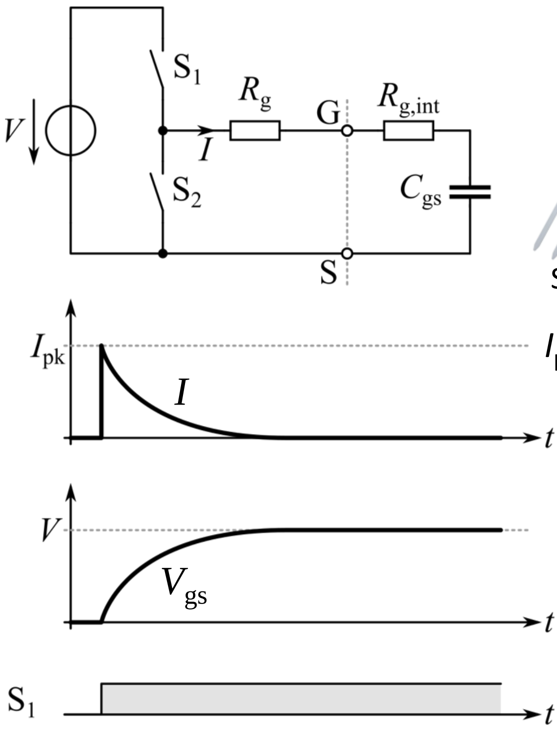

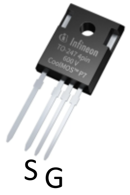

$I_{pk} = V/(R_g+R_{g,int})$

- Simplifying assumption: C_{gs} = *const.*

Simplified Gate Injection Transistor (GIT) Gate Turn-On

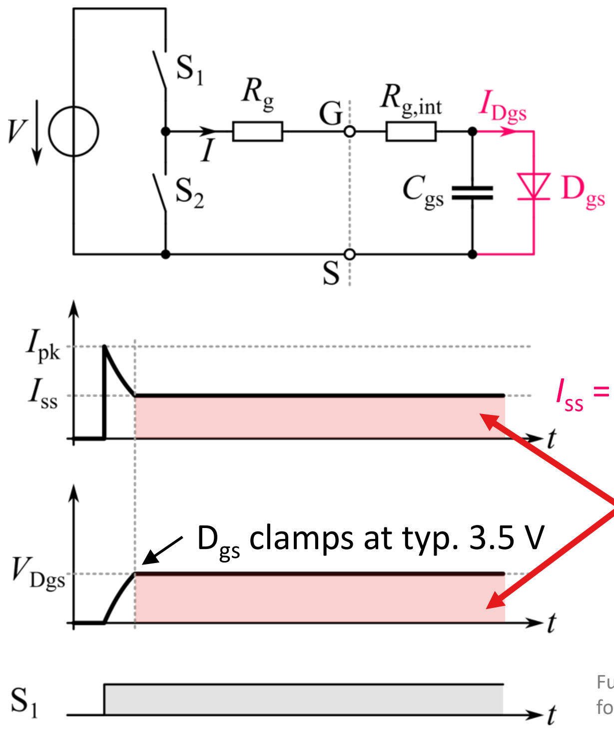

Ohmic gate contact results in diode-like behavior of GIT

$I_{ss} = I_{Dgs} = (V - V_{Dgs})/(R_g+R_{g,int})$

Losses in D_{gs}!

Further Reading: Infineon Technologies, "Gate drive solutions for CoolGaN 600V HEMTs," White Paper, Dec. 2020.

- **Requirements for GIT gate drive:**
  - **Small R_g** for fast transients (charging/discharging of C_{gs})
  - **Large R_g** during steady-state (small I_{Dgs} of a few 10 mA)

Standard RRC Gate Drive Operating Principle

- **Key idea: Capacitor C_s to decouple transient low-impedance paths**

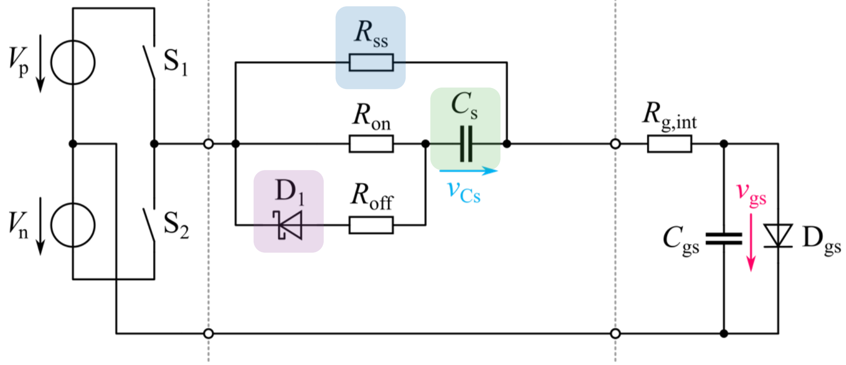

- C_s >> C_{gs} (typ.): Decoupling of High-Current Paths
- R_{ss} >> R_{on}, R_{off}: Steady-state current (milliamperes)
- D_1: Separate turn-on/turn-off gate resistors with HB driver

Note: **Dedicated driver ICs** with multiple outputs as alternative

Note: **Bipolar supply** to ensure negative v_{gs} at all times (not just transiently; relevant for CSC commutation cells)

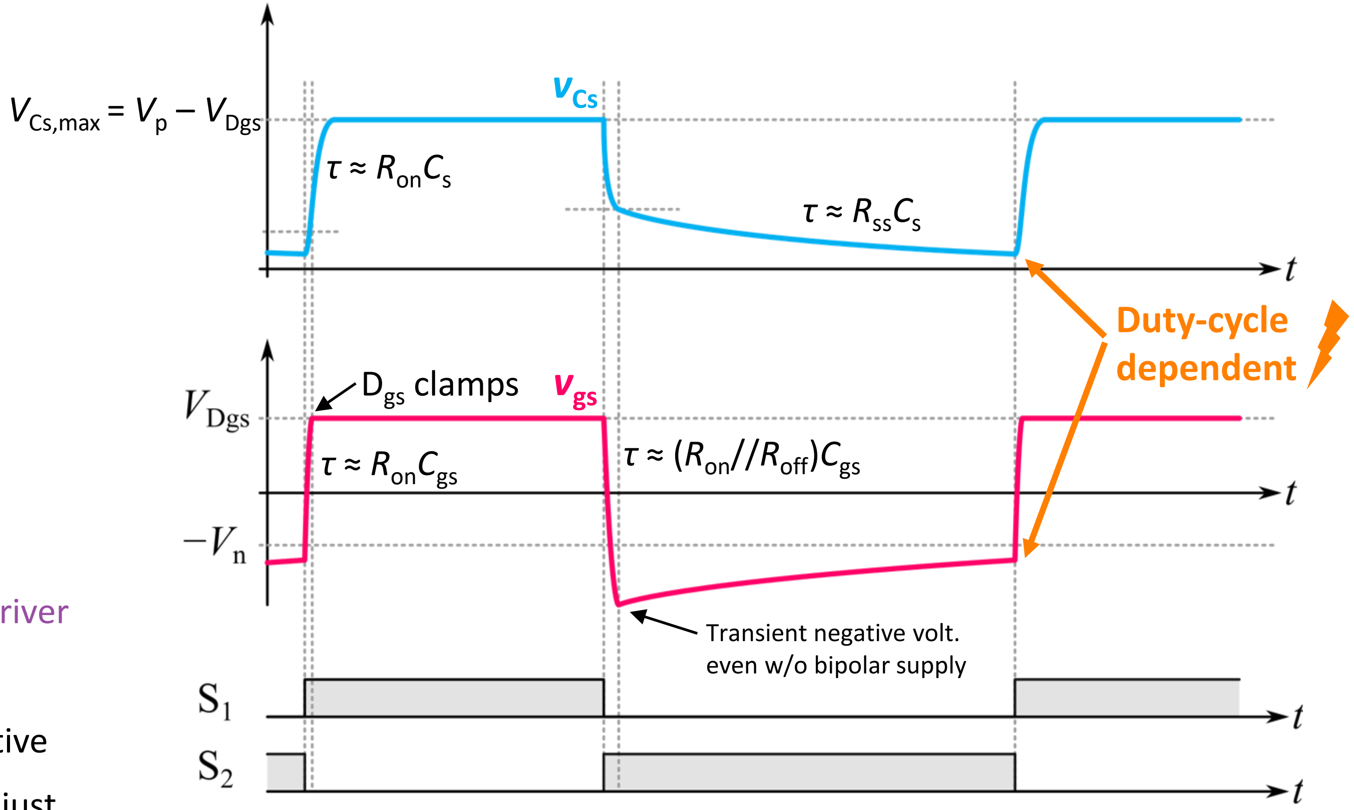

Assumptions: $R_{g,int}$ = 0 Ω, C_s >> C_{gs}, simplified gate model (C_{gs} = *const.*)

Note: unipolar supply possible; bipolar supply for better robustness against parasitic turn-on in current-source converter commutation cells (see later).

Advanced RRC Gate Drive Operating Principle

- **Key idea: Eliminate the duty-cycle dependence of dynamics**
- **Straightforward realization with standard HB driver IC and a few Schottky diodes**

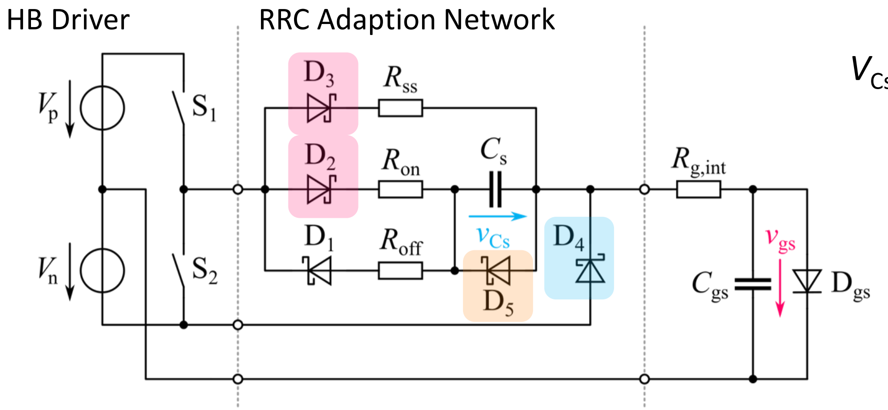

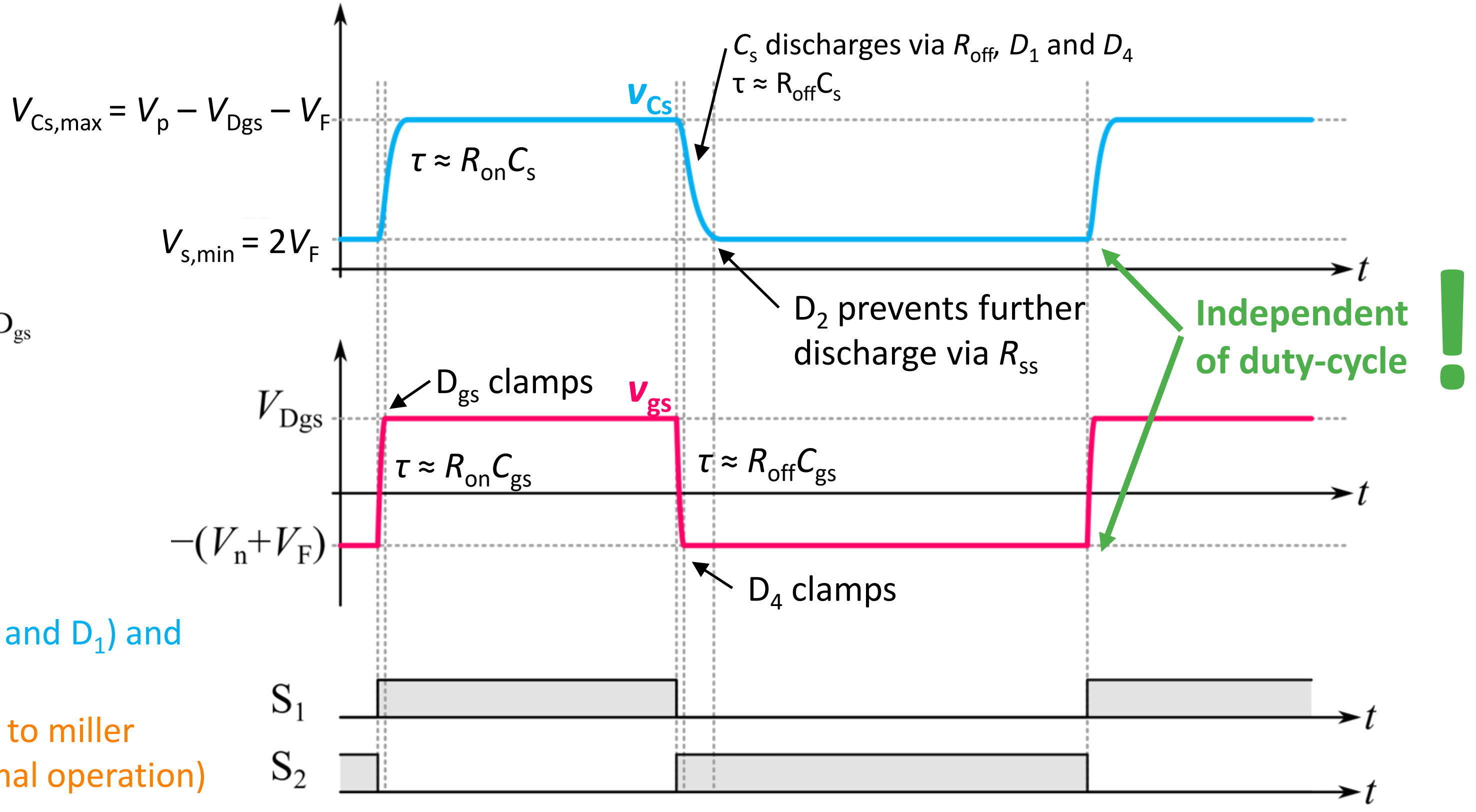

Assumptions: $R_{g,int} = 0\ \Omega$, $C_s >> C_{gs}$, simplified gate model ($C_{gs} = const.$)

- **D_2:** Prevents full discharge of C_s via R_{ss}
- **D_3:** Decouple R_{ss} during off-state
- **D_4:** Discharge path for C_s during off-state (via R_{off} and D_1) and clamping of gate to negative supply voltage
- **D_5:** Prevents negative voltage across C_s (e.g., due to miller current or other distortions; inactive during normal operation)

Further reading: D. Bortis, O. Knecht, D. Neumayr, and J. W. Kolar, "Comprehensive evaluation of GaN GIT in low- and high-frequency bridge leg applications," in *Proc. 8th IEEE Int. Power Electron. Motion Ctrl. Conf. (IPEMC-ECCE Asia)*, Hefei, China, May 2016, pp. 21–30.

Advanced RRC Gate Drive for MBDS: Realization

- **Two gates per M-BDS | Two isolated power supplies | Two control signals**
  - Mostly vertical gate loop (ca. 8…10 nH incl. package) | Adv. RRC network on TOP | HB driver sup. dec. on BOT

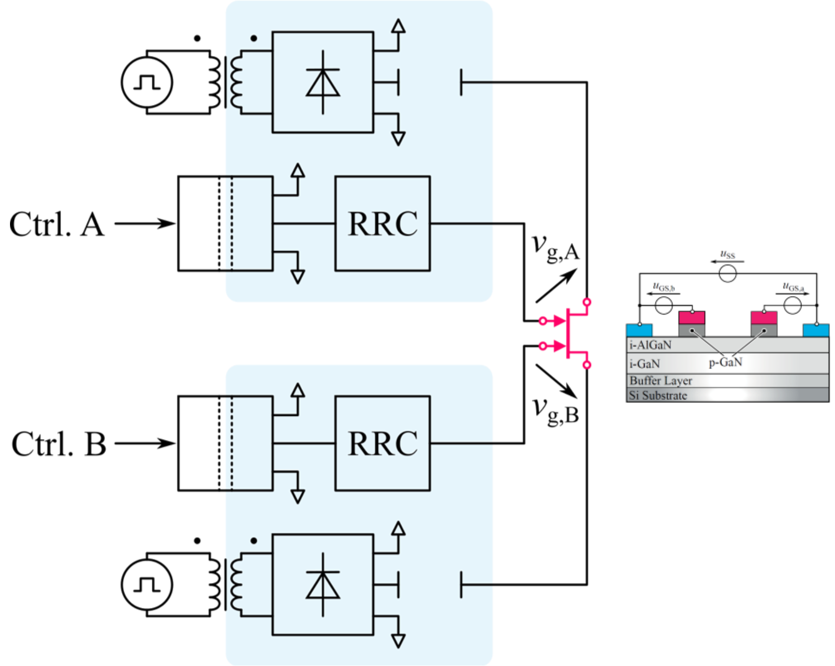

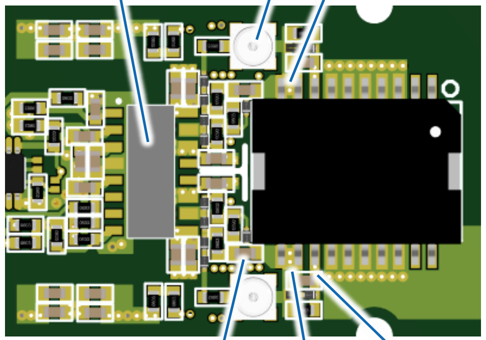

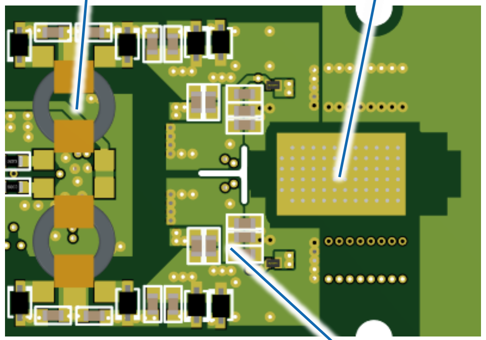

- **Remark: Integration of gate drive → Significant reduction of PCB area!**

Advanced RRC Gate Drive for MBDS: Layout / Meas.

- **Two gates per M-BDS | Two isolated power supplies | Two control signals**
  - Mostly vertical gate loop (ca. 8…10 nH incl. package) | Adv. RRC network on TOP | HB driver sup. dec. on BOT

Measured GaN M-BDS v_{gs}

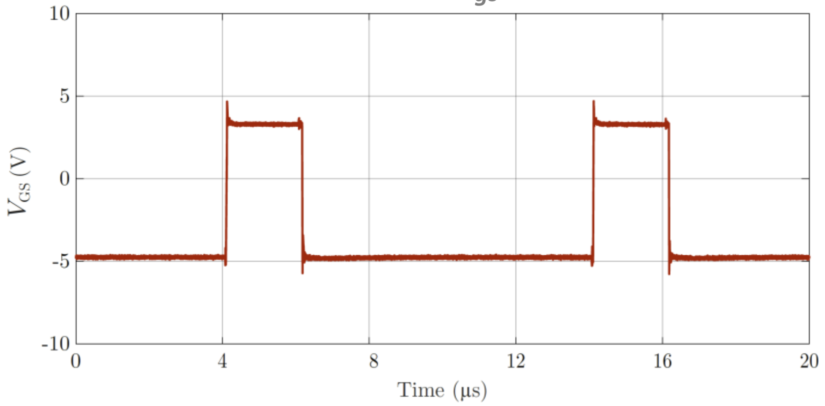

V_p = 8 V, V_n = 5 V
R_{on} = 5 Ω, R_{off} = 4.7 Ω, C_s = 2.2 nF, R_{ss} = 680 Ω

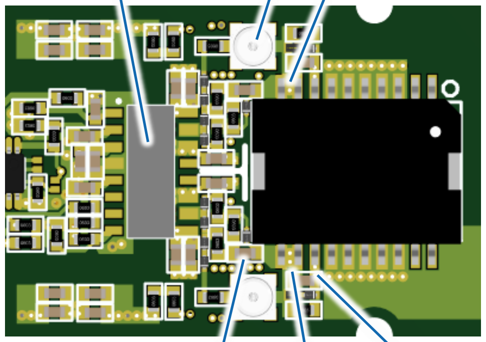

Top View

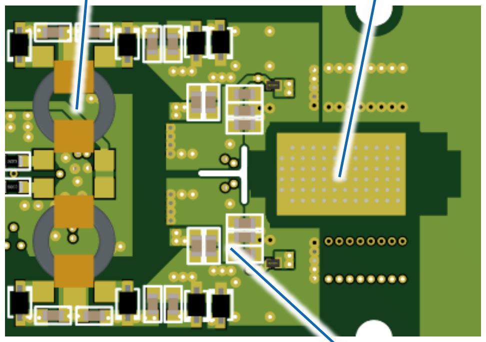

Bottom view (mirrored)

- **Remark: Integration of gate drive → Significant reduction of PCB area!**

3-Level T-Type Inverters/Rectifiers with GaN MBDSs

3-Level T-Type (TT) Main Converter Stage

- Bidirectional voltage-source AC-DC or DC-AC conv. | Basic building block for PFC rect. or motor drive inv.
- Phase-modular DC-link-referenced first LC-filter stage: DM and CM filtering

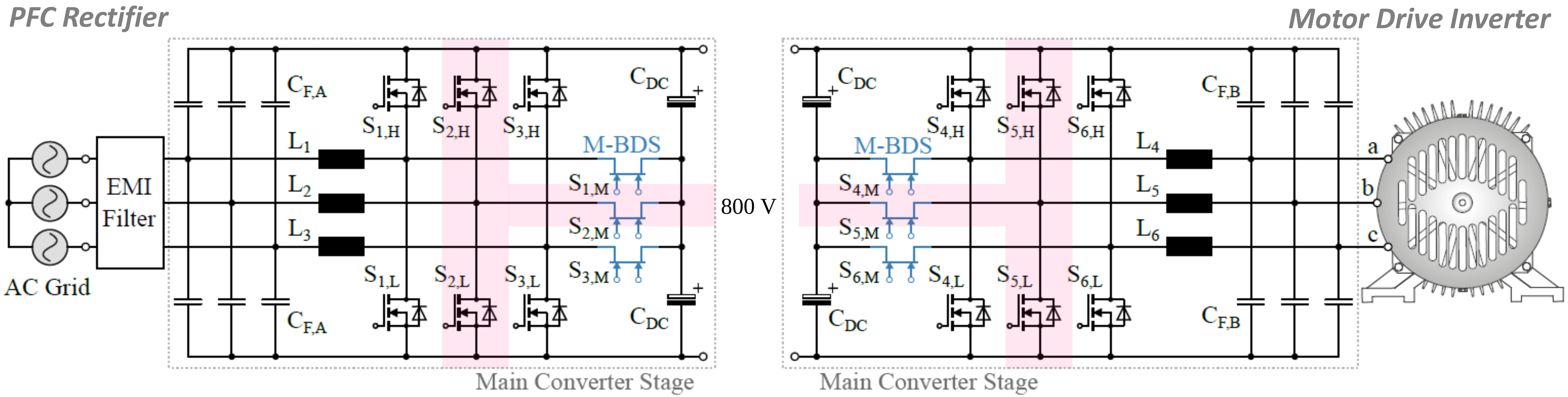

- Three-level bridge-leg via connection to DC-link midpoint: bidirectional cond. & bipolar block. → MBDS
- 800 V DC / $S_{x,H}$, $S_{x,L}$: 1200 V, 140 mΩ SiC MOSFET / $S_{x,M}$: 600 V, 140 mΩ GaN M-BDS

3-Level TT Bridge-Leg Commutation Cells

High-side commutation cell: S_H, $S_{M(A)}$

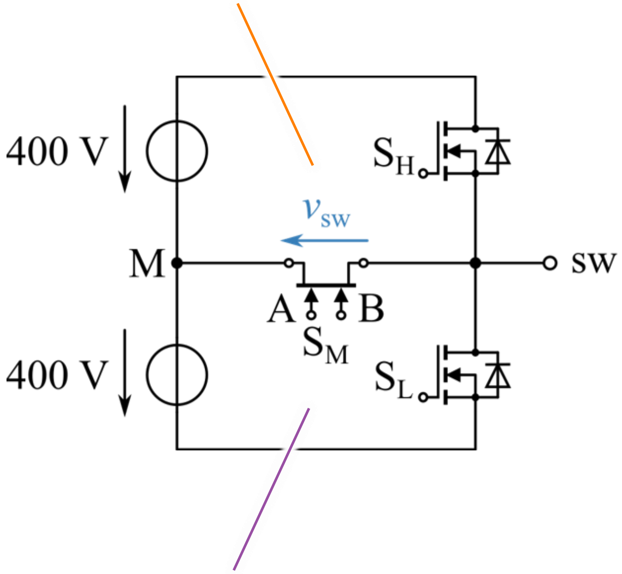

Low-side commutation cell: $S_{M(B)}$, S_L

Positive Output Voltage

→ High-side commutation cell active

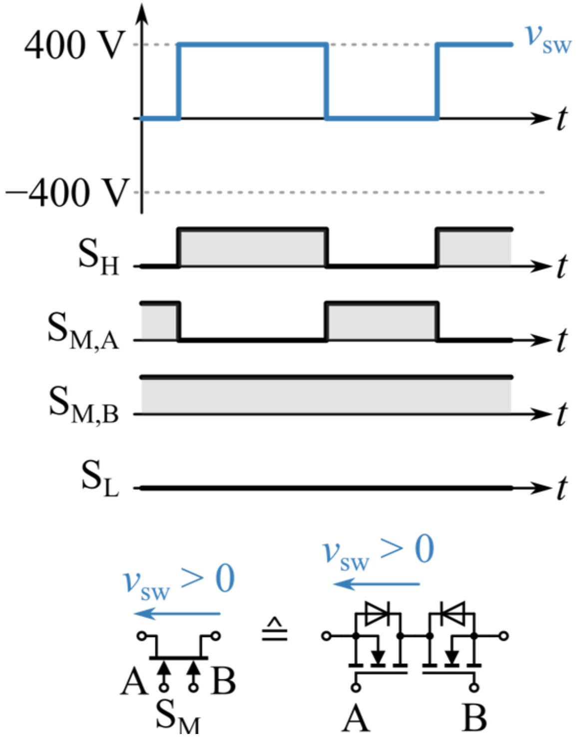

Negative Output Voltage

→ Low-side commutation cell active

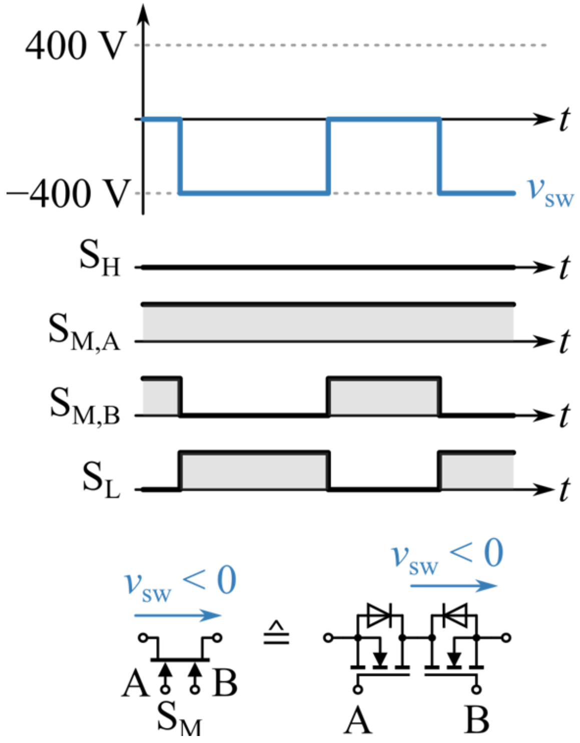

3-Level TT Bridge-Leg Evaluation Board

- **800 V DC | $S_{x,H}$, $S_{x,L}$: 1200 V, 140 mΩ SiC MOSFET (IMBG120R140M1H) | $S_{x,M}$: 600 V, 140 mΩ GaN MBDS**
- Two commutation loops: High-side & Low-side | Commutation inductance ca. 15 nH (incl. package)
- Advanced RRC gate drive with HB driver (2EDS8265HXUMA1) for M-BDS

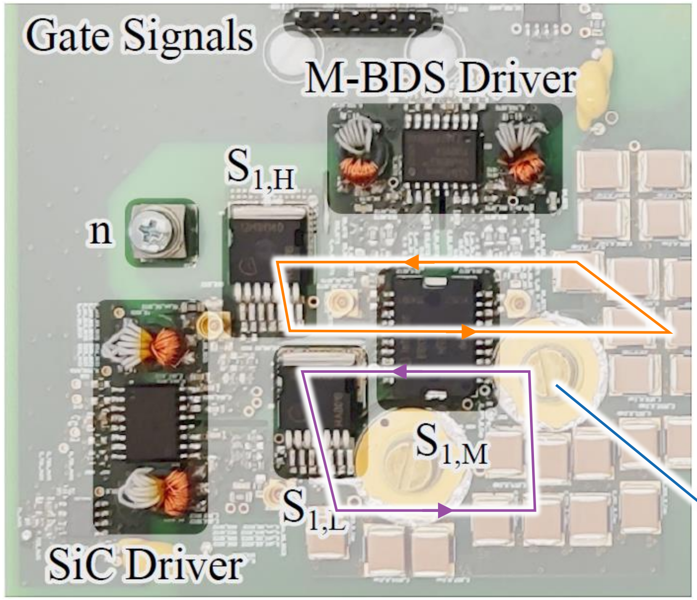

Optional coax. shunt

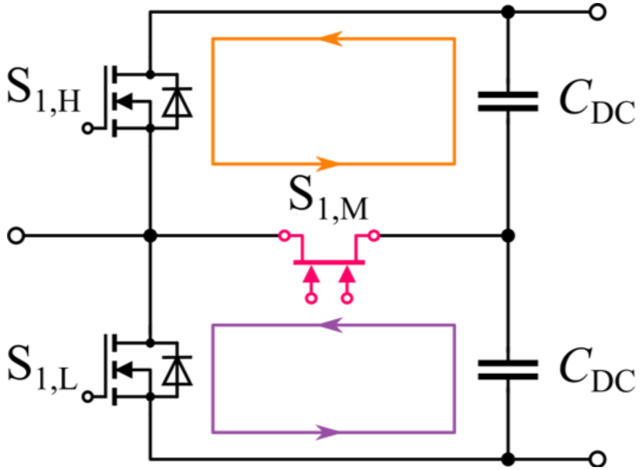

- Cooling through PCB (thermal vias) | **Top-side cooled packages** would facilitate improved layouts!

Continuous MBDS Operation at ± 400 V in CCM

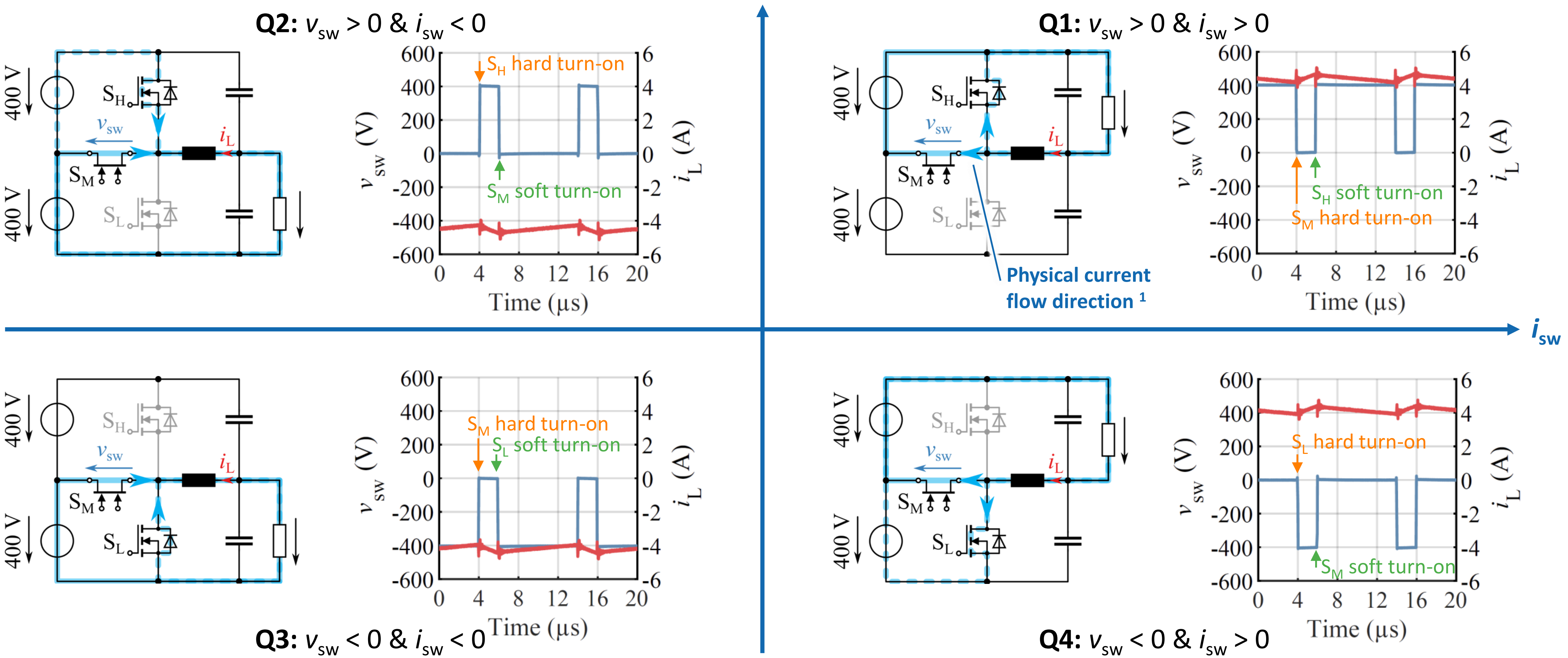

[1] Filter capacitor current not shown for better visibility

Remark: CCM and TCM Operation of TT Bridge-Leg

- CCM: Hard switching & fixed switching frequency | TCM: Soft switching & variable switching frequency

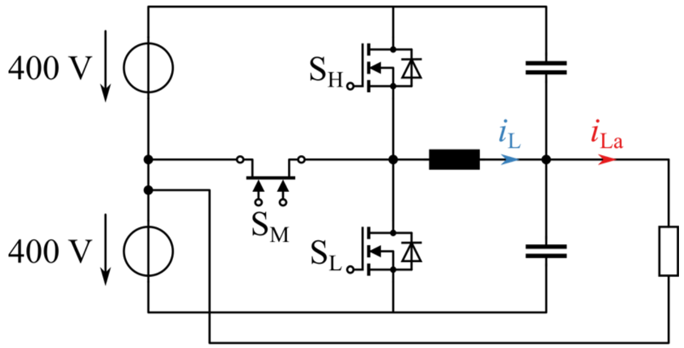

Exemplary simulations for 800 V DC and 2 kW.

CCM: Continuous Cond. Mode

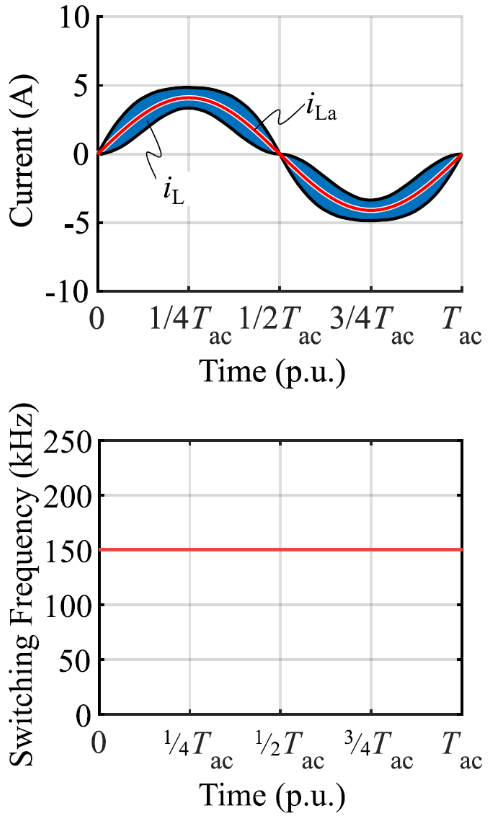

TCM: Triangular Current Mod.

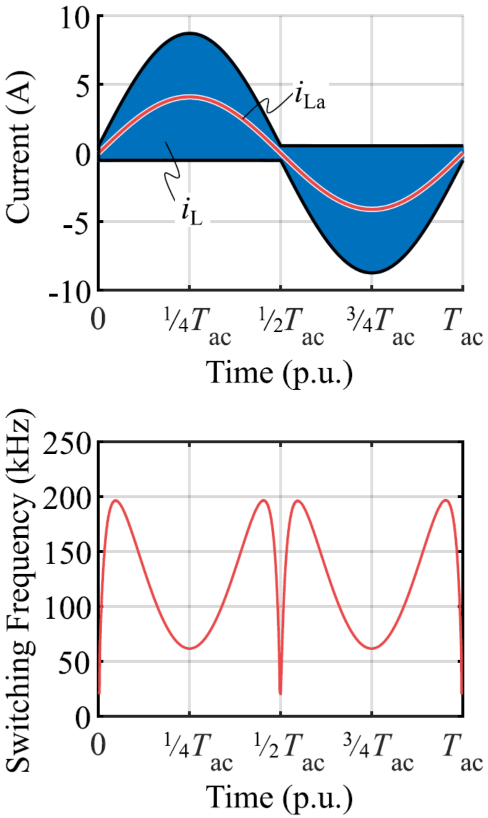

Zero-Voltage Switching (ZVS) for all transitions

Variable sw. frequency

Cont. MBDS Operation at ± 400 V with TCM (Soft-Switching)

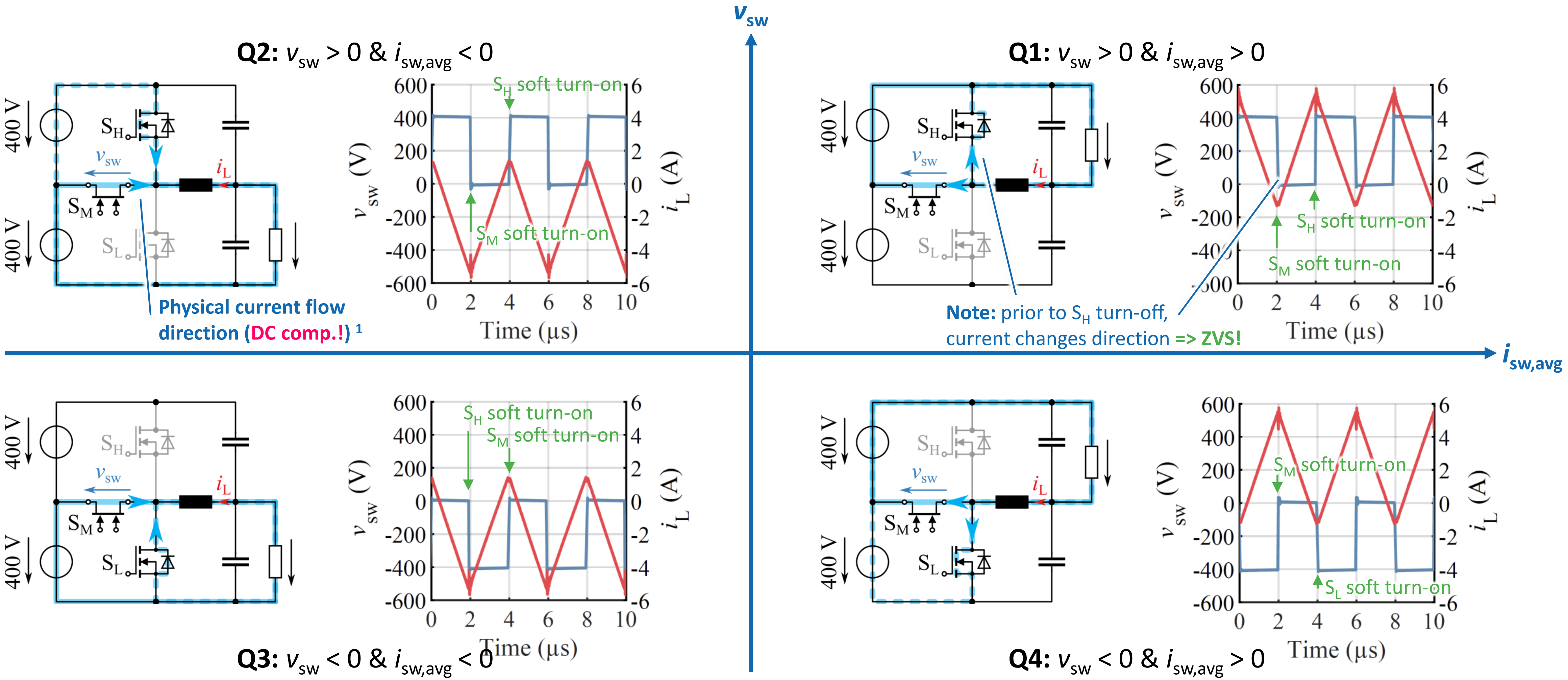

[1] Filter capacitor current not shown for better visibility

Transient Calorimetric Loss Measurement: Principle (1)

■ **Constant power dissipation into metal block**

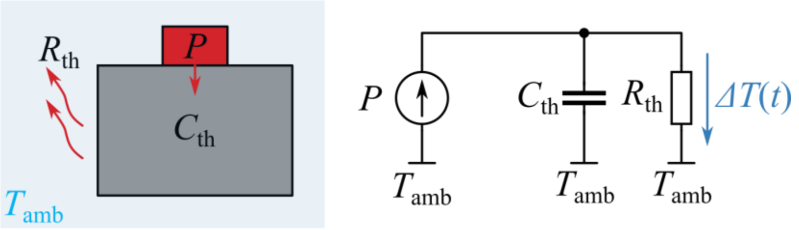

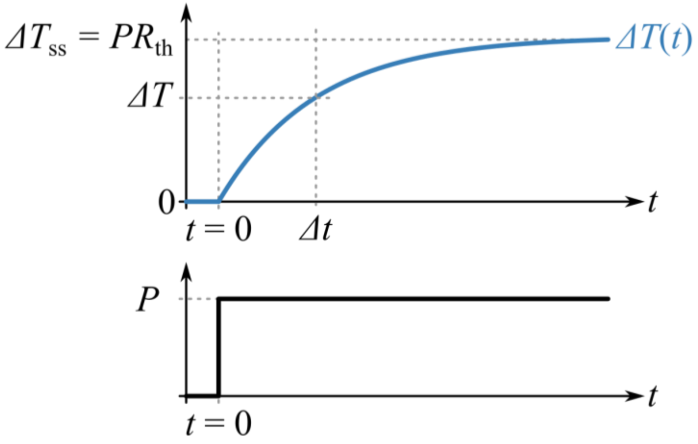

Step 1: Calibration with <u>Known</u> DC Power → Accurate electrical measurement

- Record $\Delta T(\Delta t)$ for several (at least two) known powers
- Fit model and extract model parameters C_{th} and R_{th}

$$\Delta T(\Delta t) = PR_{th} \cdot \left(1 - e^{-\frac{\Delta t}{R_{th} C_{th}}}\right)$$

Step 2: Measurement of <u>Unknown</u> Power Dissipation

- Measure time Δt to reach temperature difference ΔT
- Use calibrated model to calculate power dissipation

$$\Rightarrow \; P(\Delta T, \Delta t) = \frac{\Delta T}{R_{th} \cdot \left(1 - e^{-\frac{\Delta t}{R_{th} C_{th}}}\right)}$$

Alternative for Step 2

- Record $\Delta T(\Delta t)$ for <u>unknown</u> power dissipation P'
- Fit model with known R_{th} and C_{th} to identify P'

Transient Calorimetric Loss Measurement: Principle (2)

■ Half-bridge with identical switches

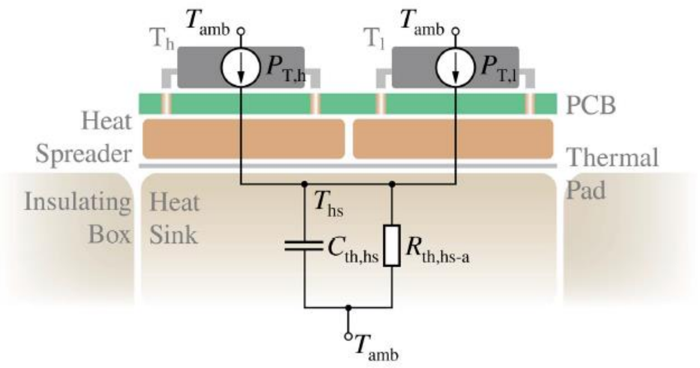

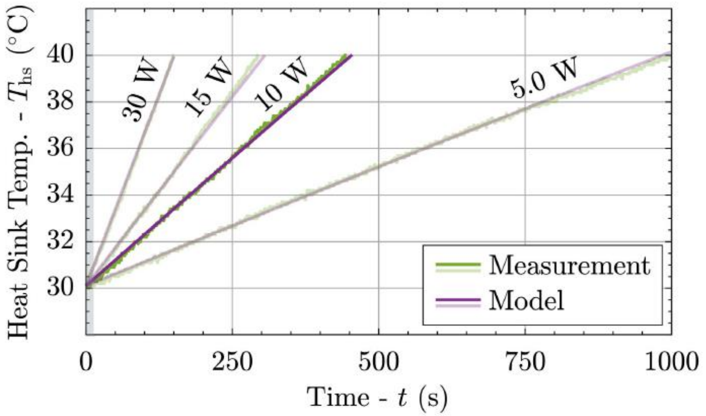

■ Switching loss extraction

- Calorimetric loss meas. gives *total* losses
- Conduction losses can be calculated:

Proxy for junction temp.

$$P_{cond} = \overbrace{R_{ds(on)}(P_{total})}^{\text{From calibration}} \cdot I_{rms}^2$$

- Switching energies follow from switching frequency

$$P_{sw} = P_{total} - P_{cond}$$

$$\boldsymbol{E_{sw}} = E_{on} + E_{off} = \frac{P_{sw}}{f_s} \quad \text{(for CCM)}$$

Half-bridge switching energy dissipation per switching period

■ Soft-switching losses

- $E_{sw} = 2E_{off}$ for TCM
- Direct & accurate meas. of residual soft-switching losses!

- Heat sink size (C_{th}) follows from desired temp. rise (resolution), meas. time, and power dissipation

Figure / Further reading: M. Guacci et al., “Experimental characterization of silicon and gallium nitride 200 V power semiconductors for modular multi-level converters using advanced measurement techniques,” *IEEE J. Emerg. Sel. Topics Power Electron.*, vol. 8, no. 3, pp. 2238–2254, Sep. 2020.

TT Bridge-Leg Switching Losses: Method (1)

- **Different device types (SiC, M-BDS) | Loss separation: Meas. individual case temp. ($T_{S1,H}$, $T_{S1,M}$, $T_{S1,L}$) and T_{HS}**

Direct dissipation to ambient ($R_{th,1}$, $R_{th,2}$, $R_{th,3}$)

Thermal cross-couplings through PCB ($R_{th,12}$, $R_{th,23}$, $R_{th,13}$)

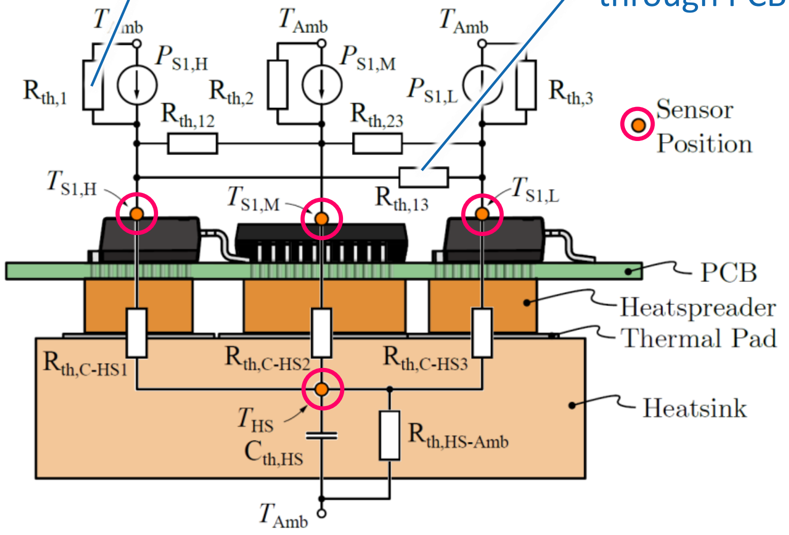

- Thermal network with 11 parameters
- Calibration with DC power injection & particle swarm fit (MATLAB)

Calibration Example

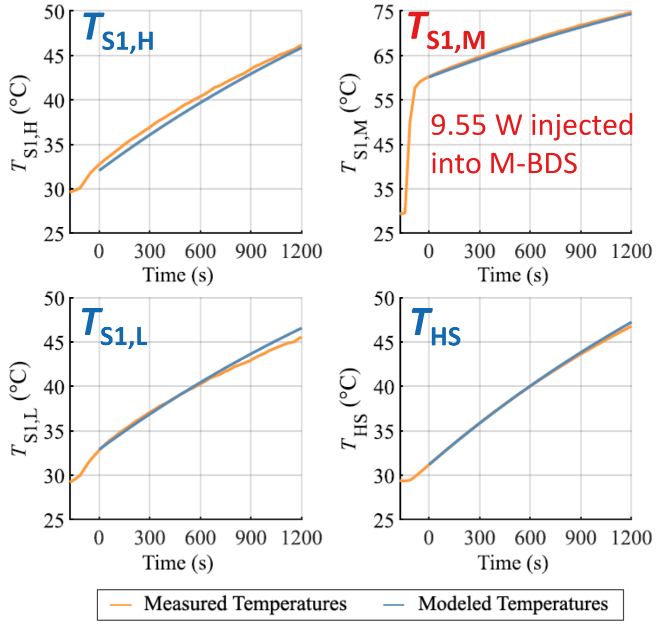

TT Bridge-Leg Switching Losses: Method (2)

- **Different device types (SiC, M-BDS) | Loss separation: Meas. individual case temp. ($T_{S1,H}$, $T_{S1,M}$, $T_{S1,L}$) and T_{HS}**

Direct dissipation to ambient ($R_{th,1}$, $R_{th,2}$, $R_{th,3}$)

Thermal cross-couplings through PCB ($R_{th,12}$, $R_{th,23}$, $R_{th,13}$)

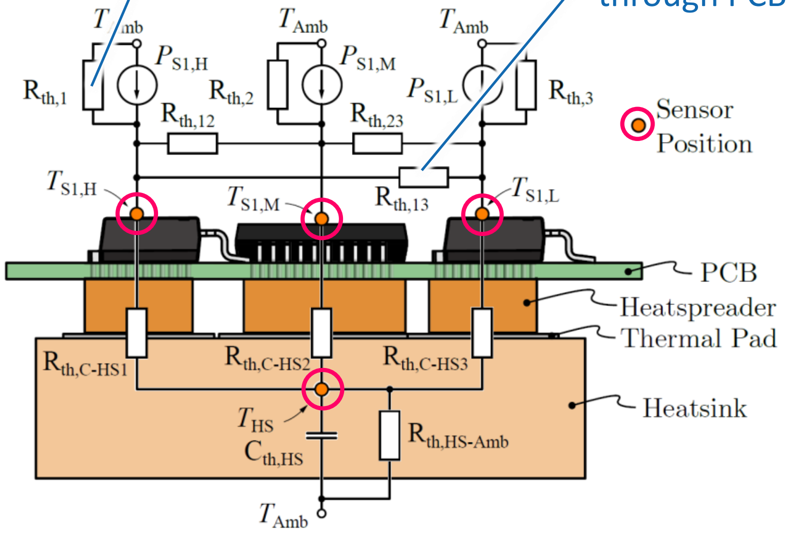

- Thermal network with 11 parameters
- Calibration with DC power injection & particle swarm fit (MATLAB)

Precision NTC temp. sensors (PS104J2)

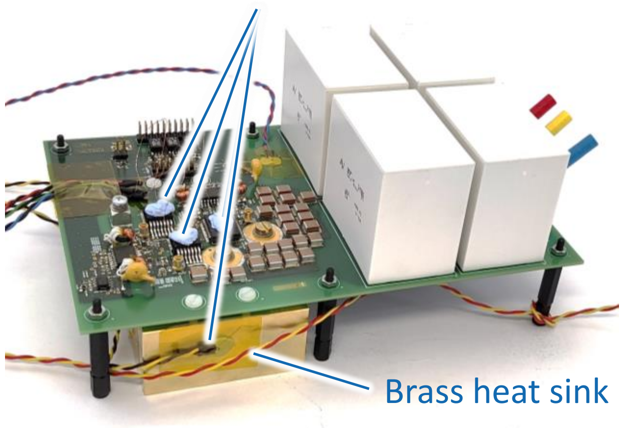

Brass heat sink

$$P_{S1,H} = \underbrace{\frac{T_{S1,H} - T_{Amb}}{R_{th,1}}}_{\text{Direct to ambient}} + \underbrace{\frac{T_{S1,H} - T_{S2,H}}{R_{th,12}} + \frac{T_{S1,H} - T_{S3,H}}{R_{th,13}}}_{\text{Cross couplings}} + \underbrace{\frac{T_{S1,H} - T_{HS}}{R_{th,C-HS1}}}_{\text{To heat sink}}$$

TT Bridge-Leg Switching Losses: Results

Calibration Data / Accuracy

- Injected DC power vs. calorimetric measurement

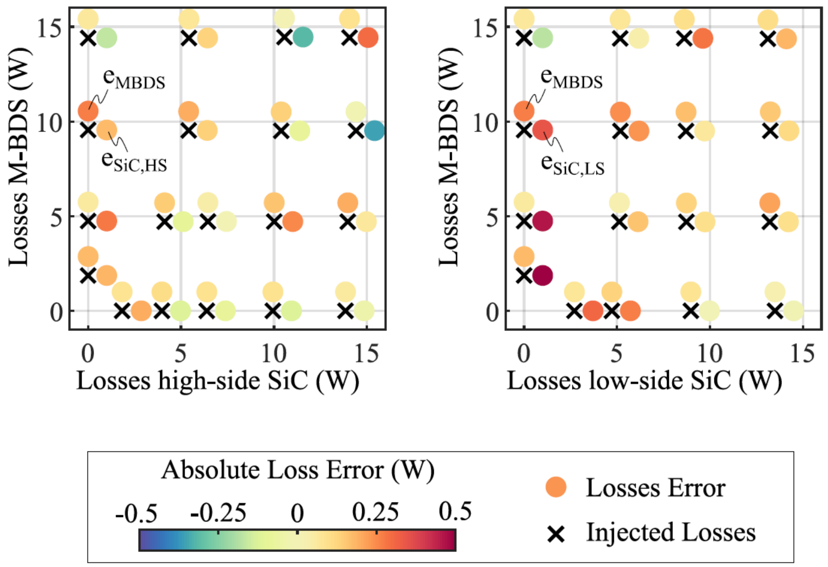

Measured Hard- and Soft-Switching Losses

1200 V, 140 mΩ SiC (IMBG120R140M1H)

600 V, 140 mΩ GaN MBDS

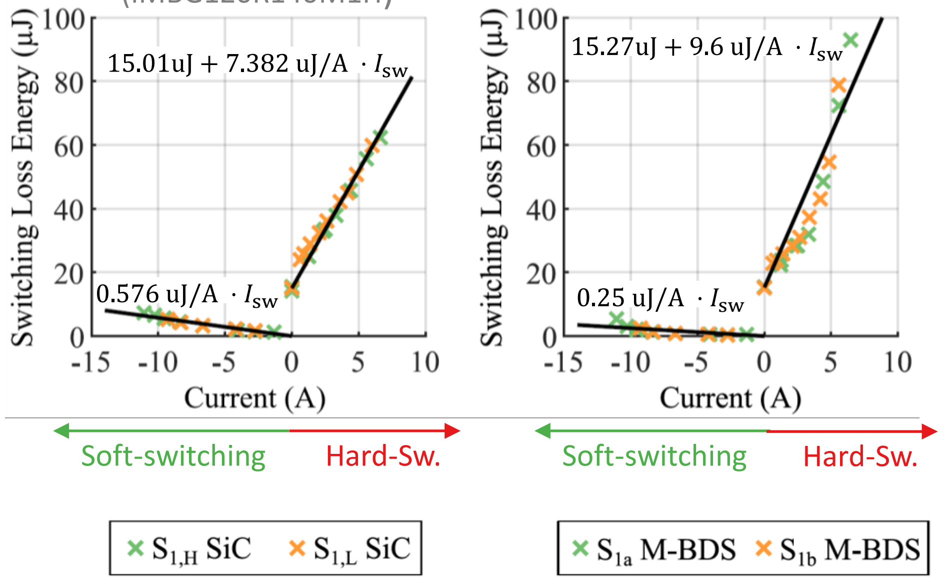

TT Main Converter Stage Performance Evaluation

- **CCM: Sweet spot at 2 kW design power: η > 99 % at ρ > 15 kW/dm^3**
- **TCM: Favorable for lower design powers, e.g., 1 kW**

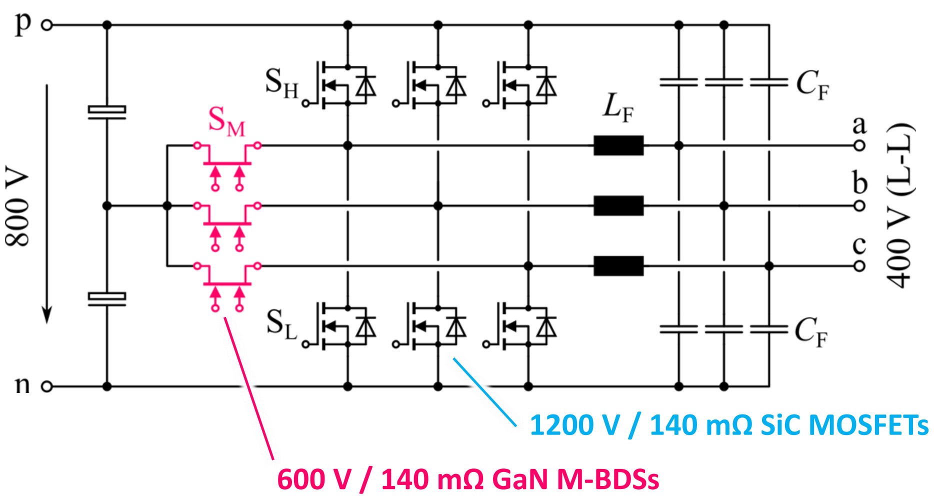

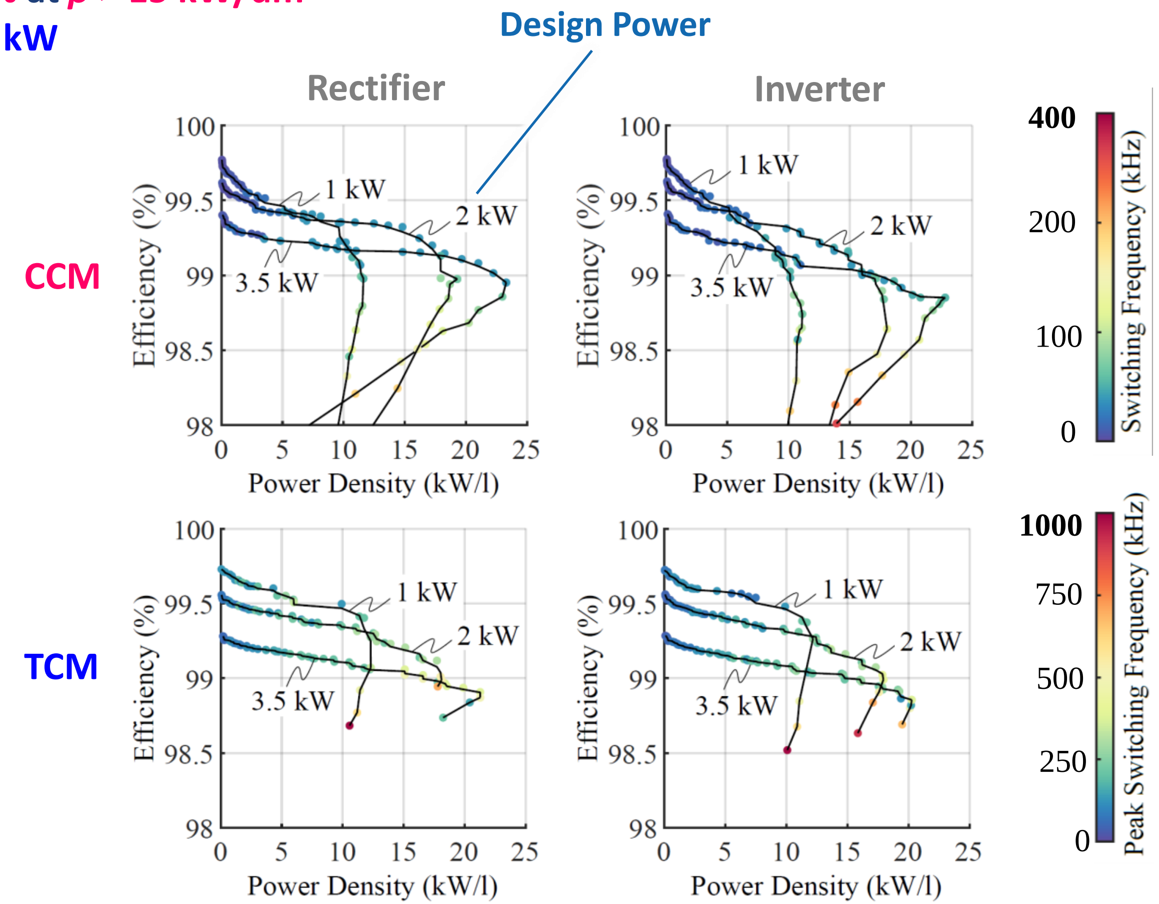

- **Specifications / Modeling**
  - T_j = 125 °C, T_{amb} = 45 °C / heat sink volume: CSPI = 15 W/(dm^{3}K)
  - $\Delta i_{LF,pp}$ = 30 % (CCM), $\Delta v_{CF,pp}$ = 2 %,
  - Pareto-optimal inductors (N87, KoolMu)
  - Inverter or rectifier designs with cosϕ = ± 1

Further Reading: F. Vollmaier, N. Nain, J. Huber, J. W. Kolar, K. K. Leong, and B. Pandya, "Performance evaluation of future T-Type PFC rectifier and inverter systems with monolithic bidirectional 600V GaN switches," in *Proc. IEEE Energy Conv. Congr. Expo. (ECCE)*, Vancouver, Canada, Oct. 2021, pp. 5297–5304. doi: 10.1109/ECCE47101.2021.9595422.

AC-AC Current-Source Converters with MBDSs

MBDS Commutation Cell for AC-AC CSC and DMC

AC-AC Current-Source Converter (CSC)

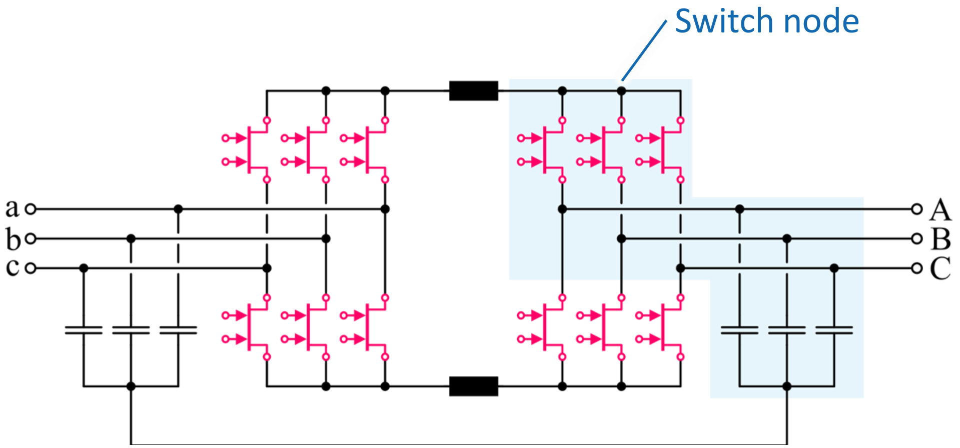

- 4 x Basic commutation cell

AC-AC Direct Matrix Converter (DMC)

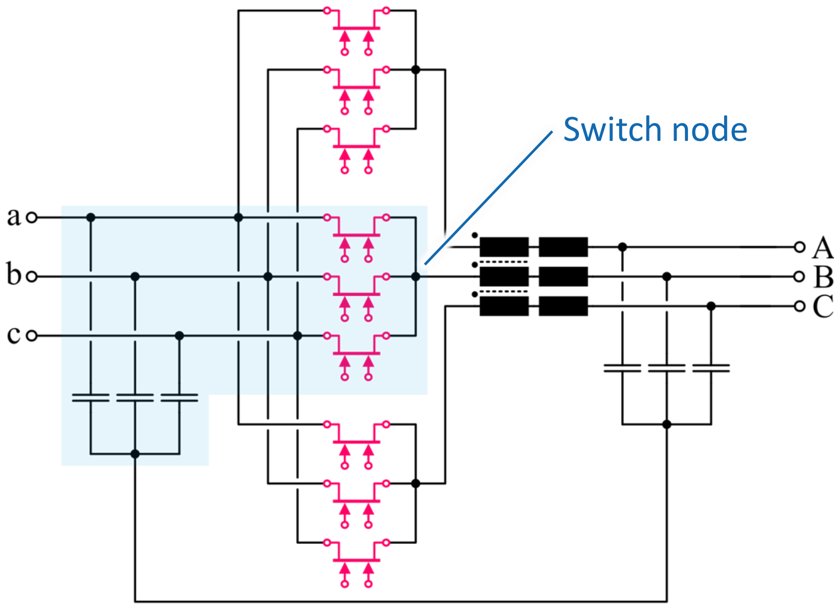

- 3 x basic commutation cell

MBDS Commutation Cell Test PCB: Commutation Loops

- **Commutation voltages: Line-to-line AC voltages | Commutation capacitors: Two AC-side filter capacitors**

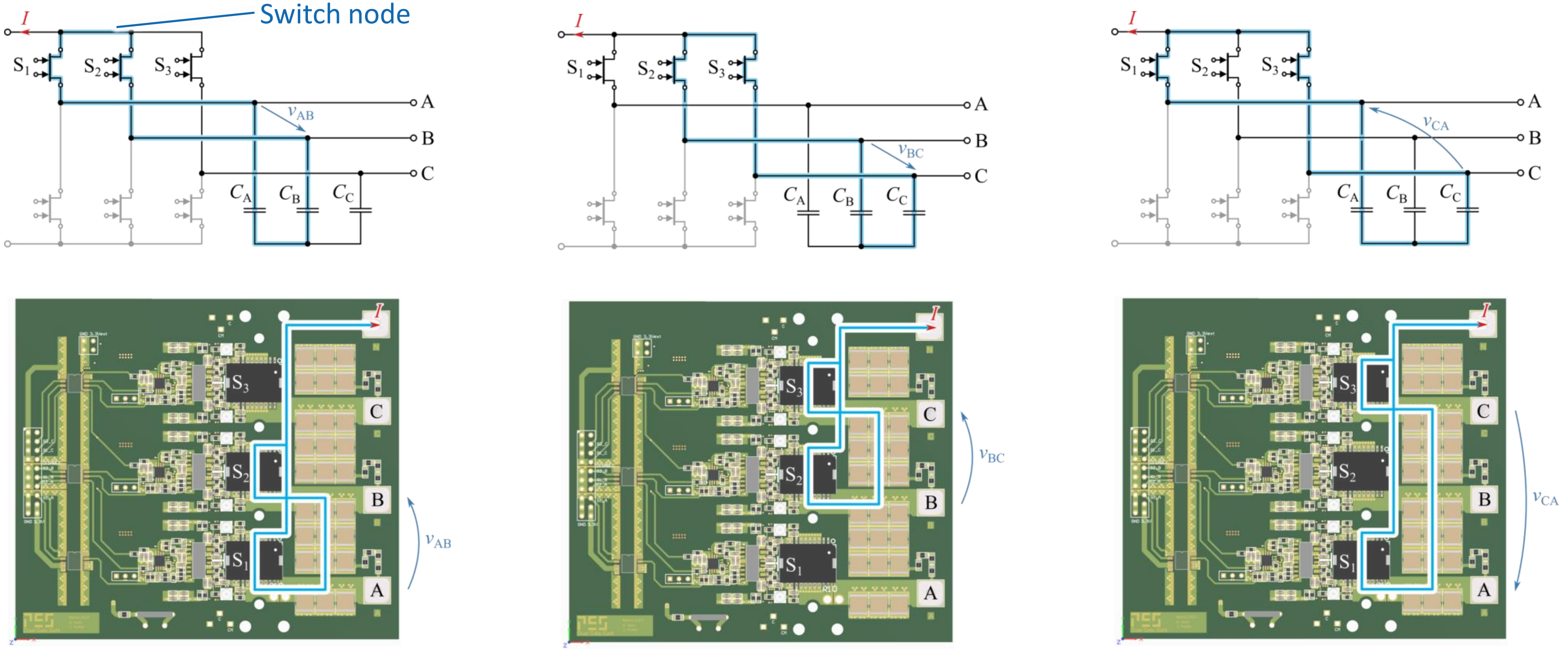

- Bottom-cooled package: Mostly lateral commutation loops (approximate loops shown)

MBDS Comm. Cell Test PCB: Half-Bridge Configuration

- **DUT operation in all four quadrants by reconfiguring voltage source / load**
- DC supply between B-C or C-B (voltage polarity, ± 400 V) | Load between p-C or p-B (current direction)

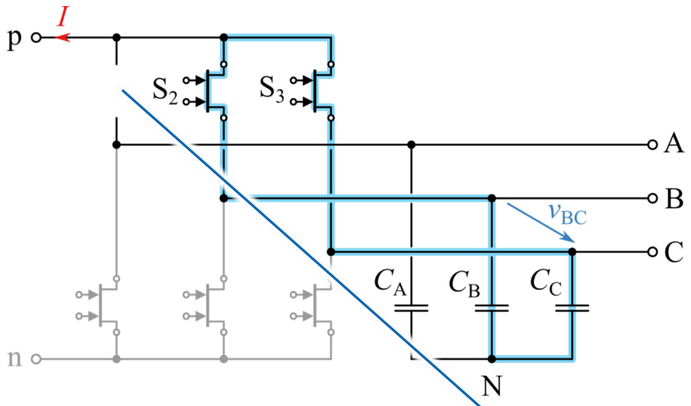

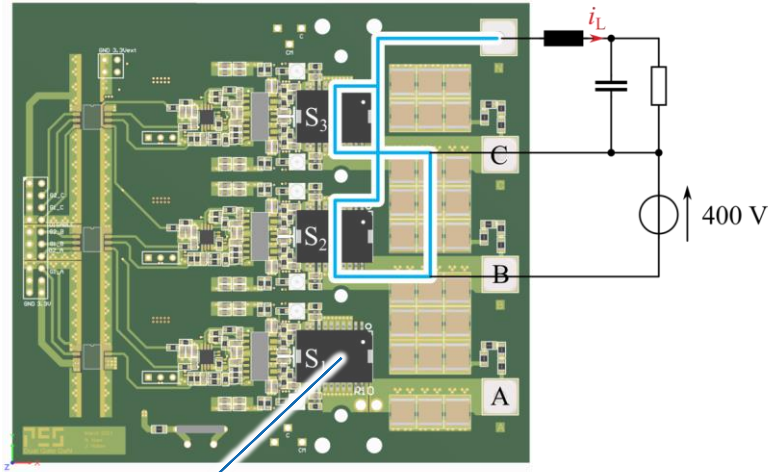

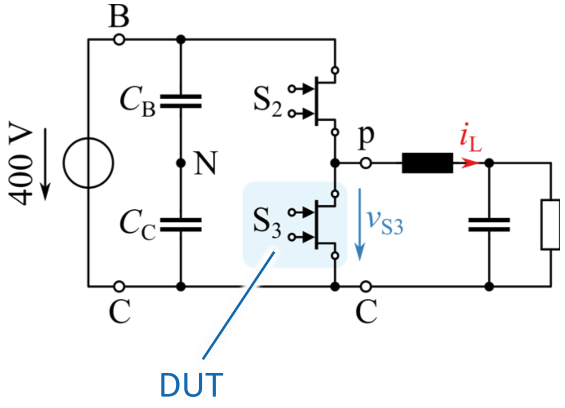

S_1 not placed for initial meas.

- Impact of S_1 presence discussed later!

Remark: 4-Step Commutation (Positive Current)

- Ensure current path & avoid DC voltage short-circuit | Current-direction-dependent gating seq (pos. cur. shown)

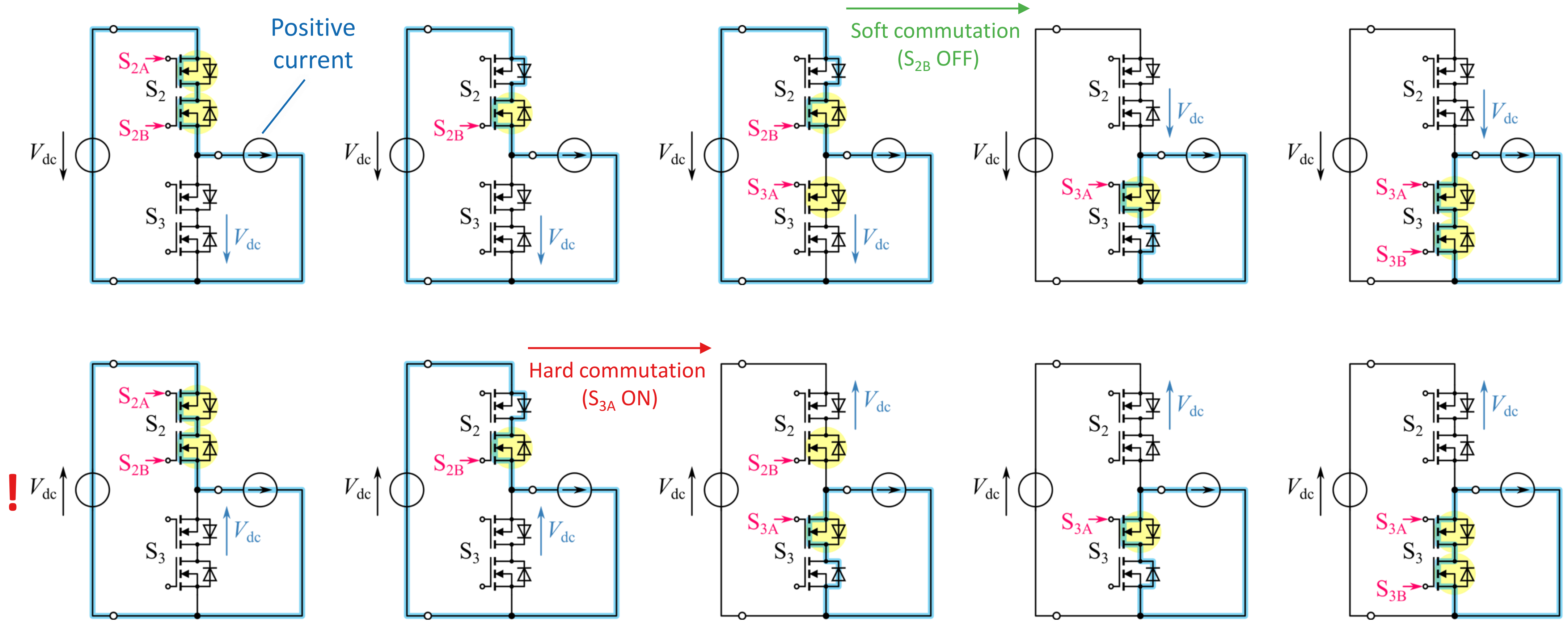

- Note: voltage-polarity-dependent commutation sequences possible, too

Remark: 4-Step Commutation (Negative Current)

- **Ensure current path & avoid DC voltage short-circuit | Current-direction-dependent gating seq (neg. cur. shown)**

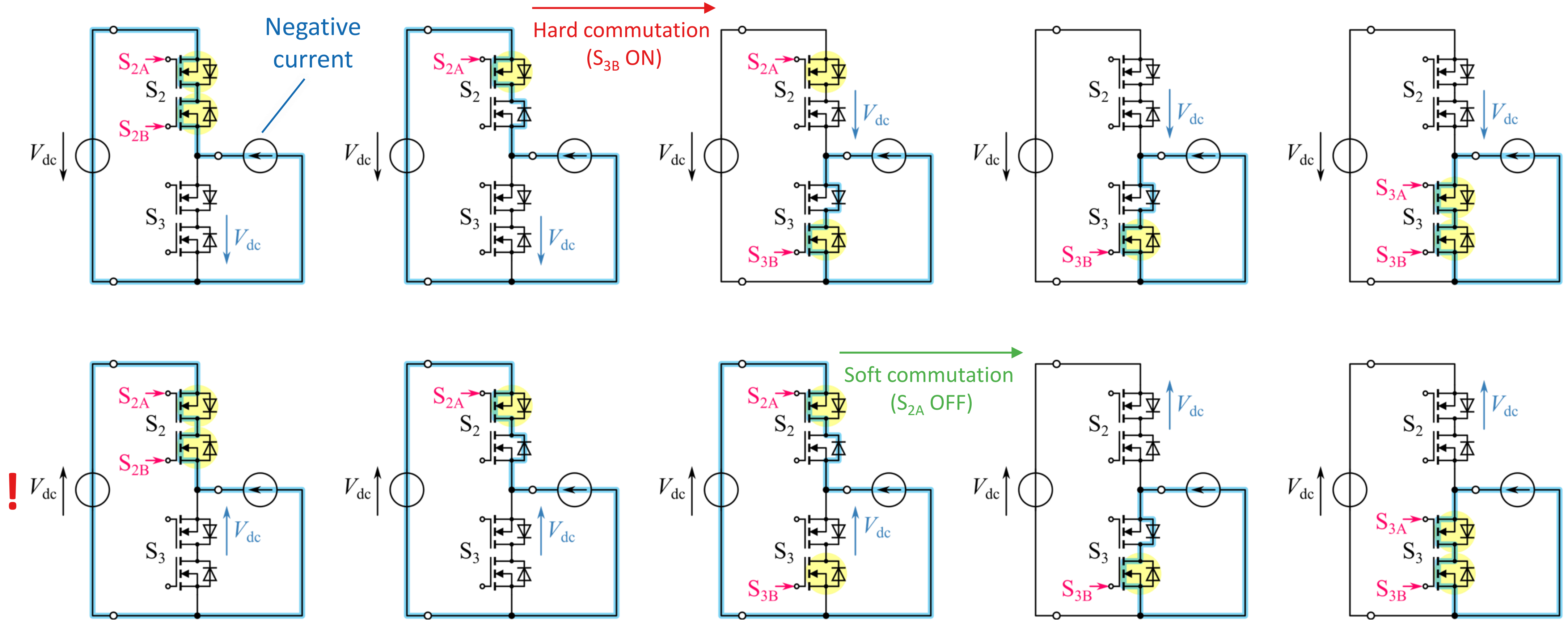

- Note: voltage-polarity-dependent commutation sequences possible, too

Continuous MBDS Half-Bridge Operation at ± 400 V

v_{S3}

Q2: $v_{S3} > 0$ & $i_{S3} < 0$

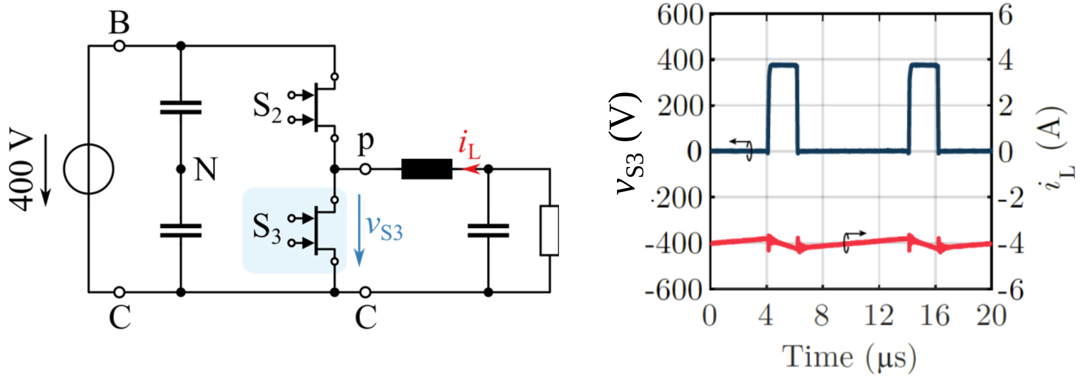

Q1: $v_{S3} > 0$ & $i_{S3} > 0$

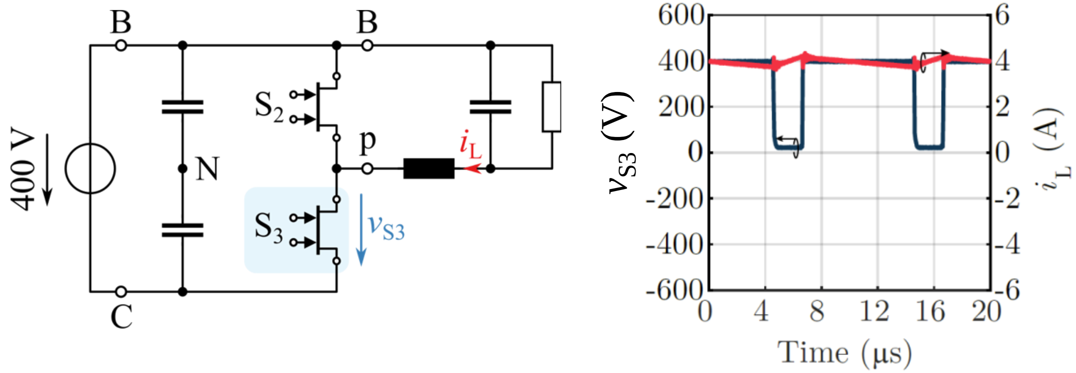

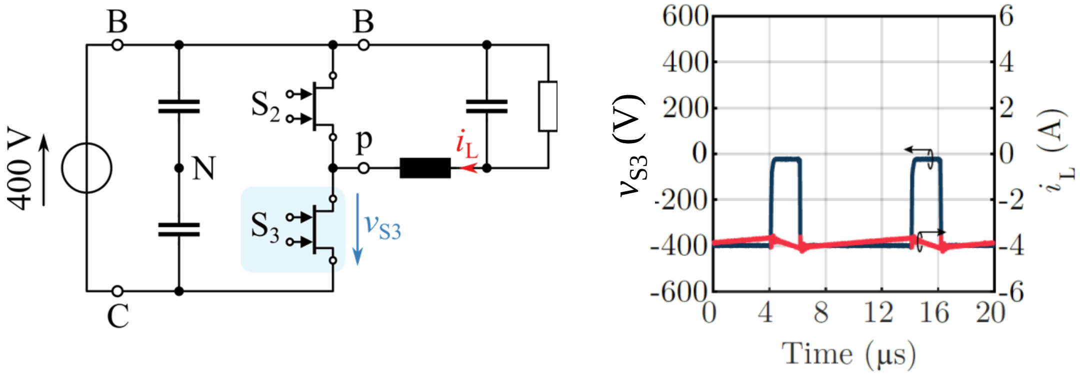

Q3: $v_{S3} < 0$ & $i_{S3} < 0$

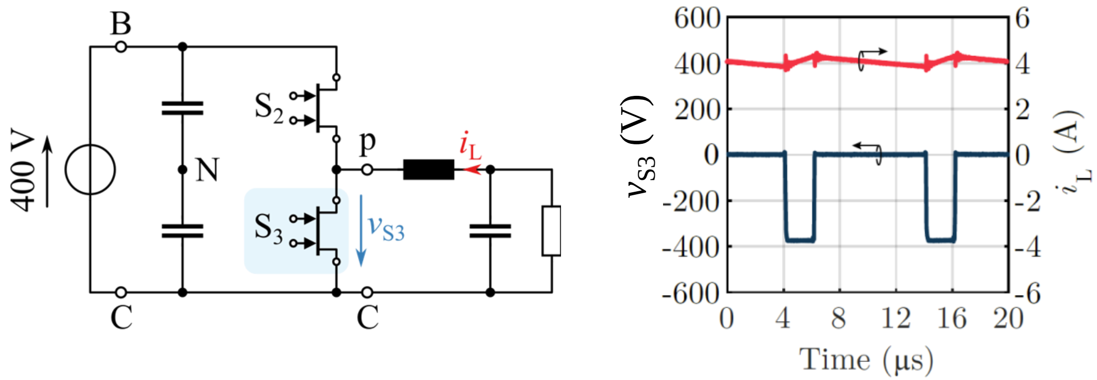

Q4: $v_{S3} < 0$ & $i_{S3} > 0$

MBDS Half-Bridge Switching Loss Characterization

- **Transient calorimetric method w. loss separation (see TT above) | 4-Step current-based commutation seq.**

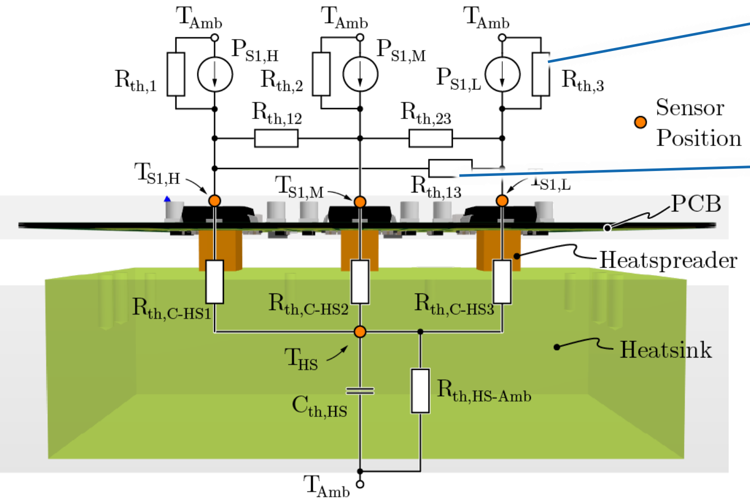

Direct dissipation to ambient ($R_{th,1}$, $R_{th,2}$, $R_{th,3}$)

Thermal cross-couplings through PCB ($R_{th,12}$, $R_{th,23}$, $R_{th,13}$)

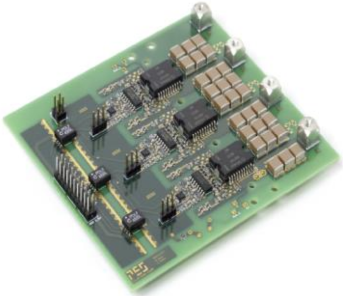

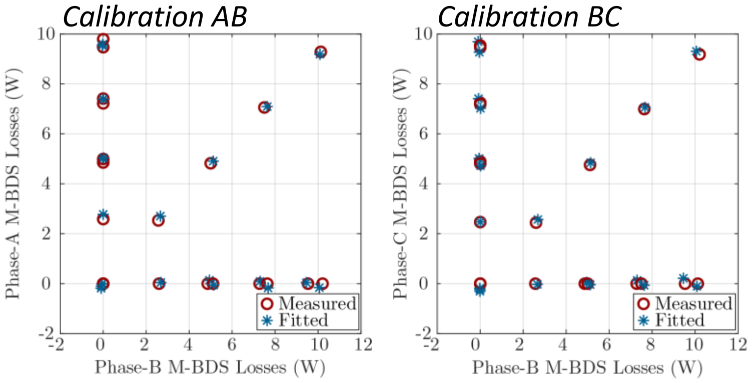

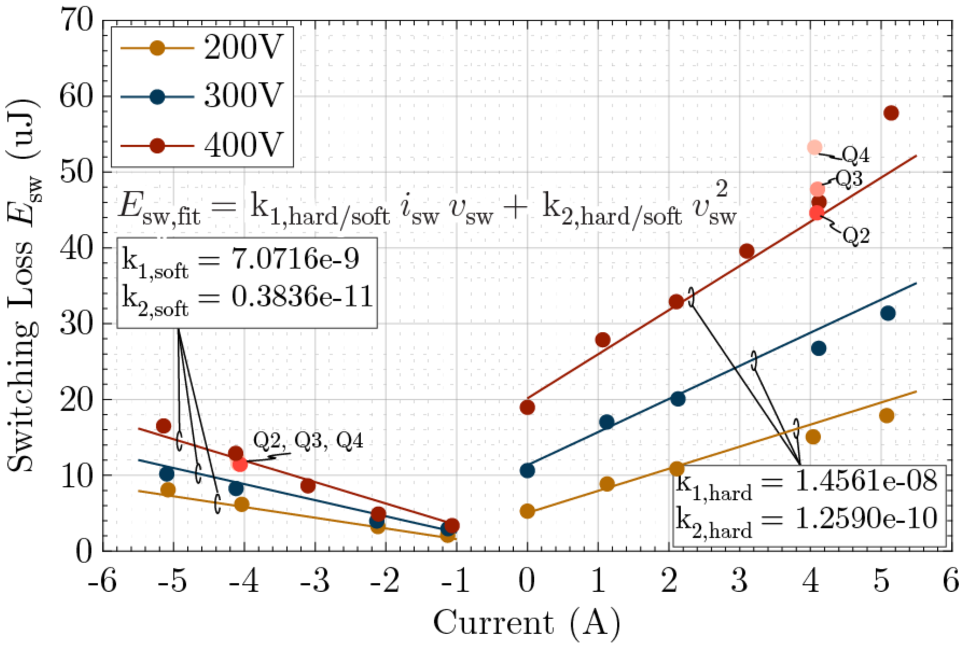

Remark: Passive Toggling of Comm. Cell's 3rd Switch (1)

- Three switches connected to common switch node
- Example: Commutation from S_1 to S_2 => Charging/discharging of $C_{oss}(S_3)$ creates additional losses[1]

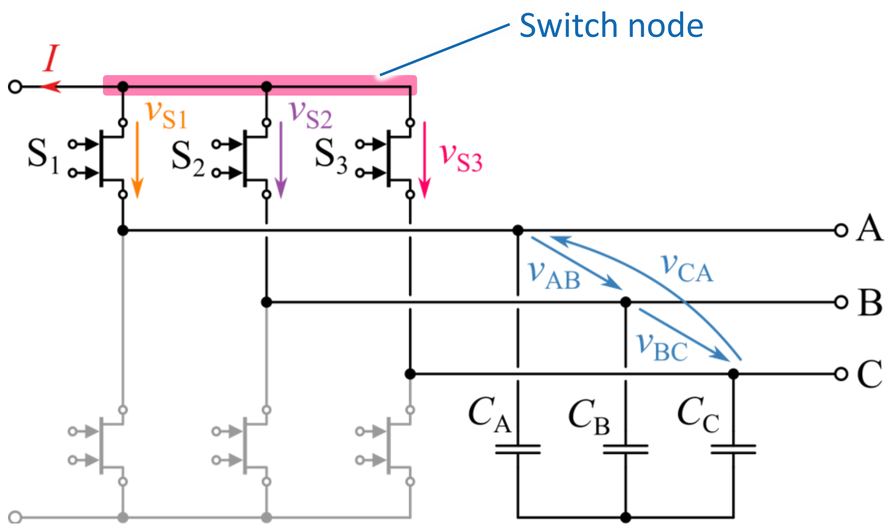

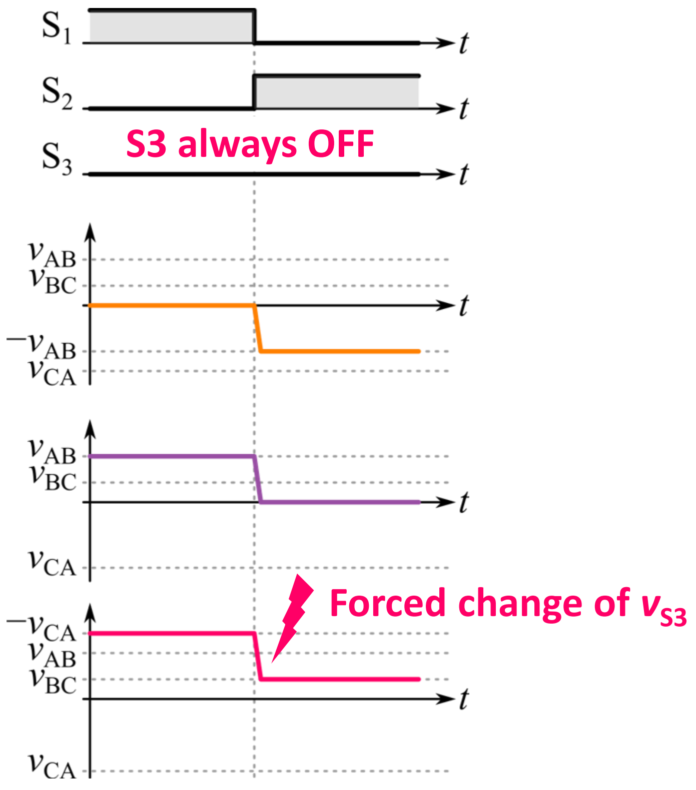

- Risk of parasitic turn-on (dv/dt-induced): Ensure neg. gate. volt.!

[1] Note: similar effect also in TT bridge-legs

Remark: Passive Toggling of Comm. Cell's 3rd Switch (2)

- **Transient calorimetric method w. loss separation (see TT above) | 4-Step current-based commutation seq.**
- **3rd switch loss contribution estimation w. datasheet parameters | E_{passive} dissipated in active switches!**

$$E_{\text{passive}}(v_x, v_y) = [Q_{\text{oss}}(v_y) - Q_{\text{oss}}(v_x)] \cdot v_y - [E_{\text{oss}}(v_y) - E_{\text{oss}}(v_x)]$$

$v_x = v_{\text{passive}}$ before sw. transient
$v_y = v_{\text{passive}}$ after sw. transient

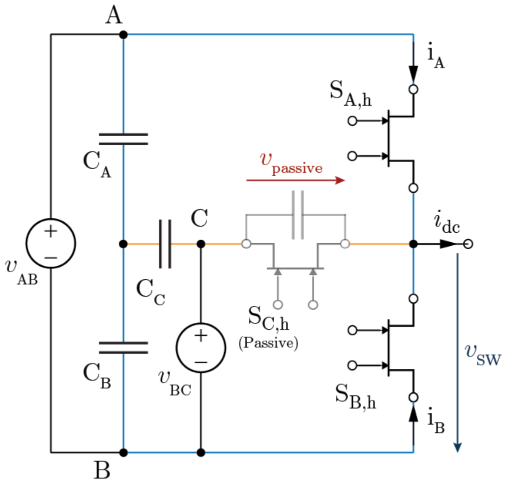

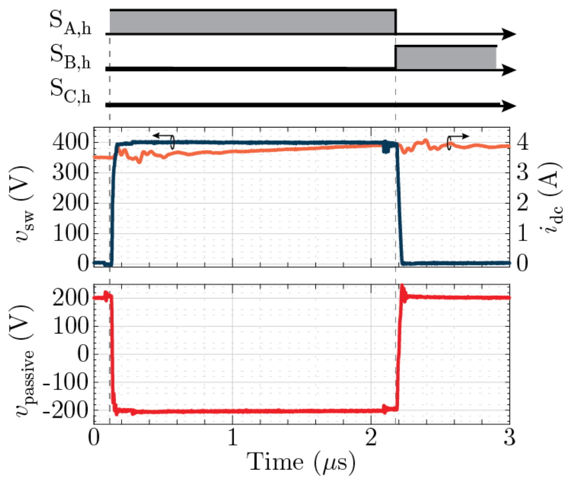

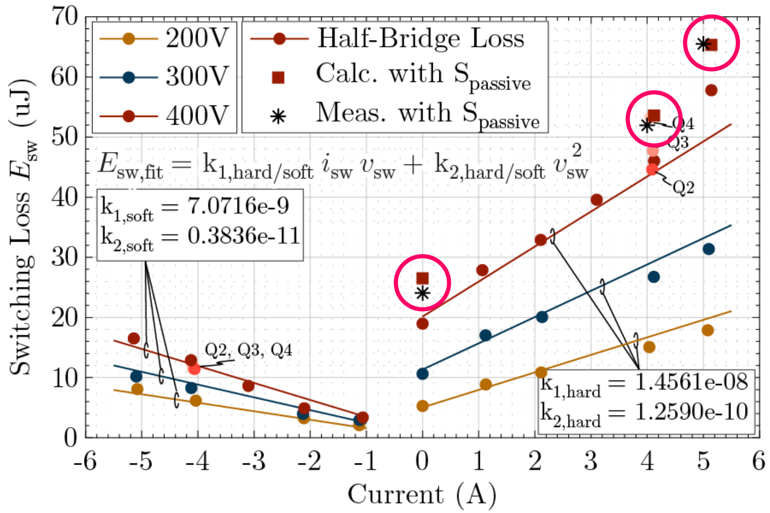

- Datasheet-based estimation of E_{passive} with error < 10 %
- Note: Minor impact (loss increase) in actual CSC operation (modulation, varying switched voltage)

Further Reading: N. Nain, D. Zhang, J. Huber, J. W. Kolar, K. K. Leong, and B. Pandya, "Synergetic control of three-phase AC-AC current-source converter employing monolithic bidirectional 600 V GaN transistors," *Proc. 22nd IEEE Control and Modeling for Power Electron. Workshop (COMPEL),* Cartagena, Colombia, Nov. 2021. doi: 10.1109/COMPEL52922.2021.9646006.

Three-Phase AC-AC Converter Topologies (1)

■ **Current-Source Converter**
- Application of **MBDSs | 12 Switches**
- Multi-step commutation
- Low filter volume
- **Buck-boost** functionality

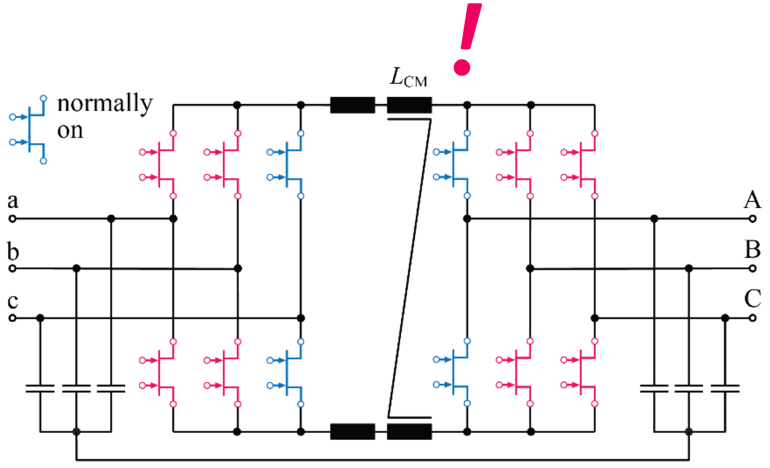

- Challenging overvoltage protection

■ **Direct Matrix Converter**
- Application of **MBDSs | 9 Switches**
- Multi-step commutation
- Complex space-vector modulation
- Limited to **buck operation (!)**

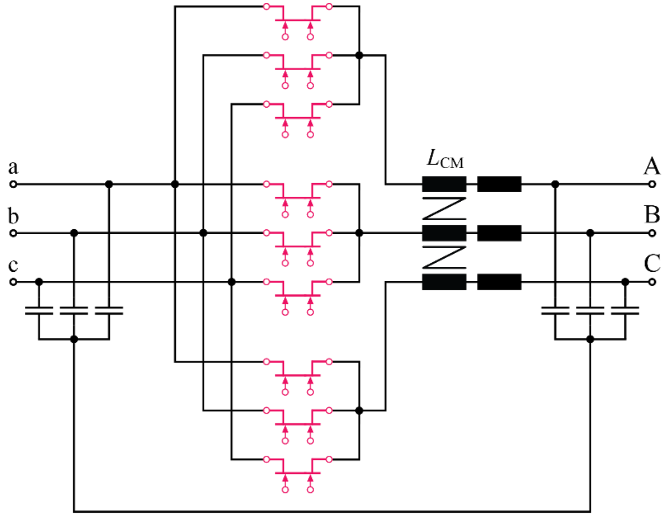

- Challenging overvoltage protection

Three-Phase AC-AC Converter Topologies (2)

Current-Source Converter (CSC)

- Application of **MBDSs**
- Complex multi-step commutation
- Fewer magnetic components

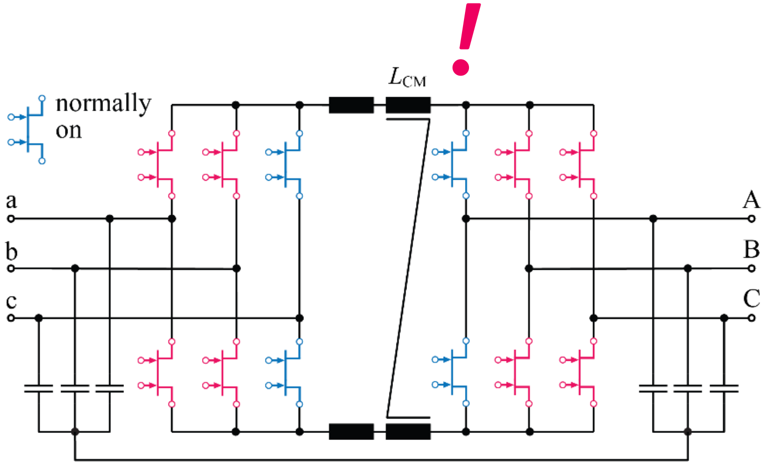

- Challenging overvoltage protection
- Pot. limited control dynamics

Voltage-Source Converter (VSC)

- **Standard** bridge legs
- Low-complexity commutation
- Defined semiconductor voltage stress
- Facilitates DC-link energy storage

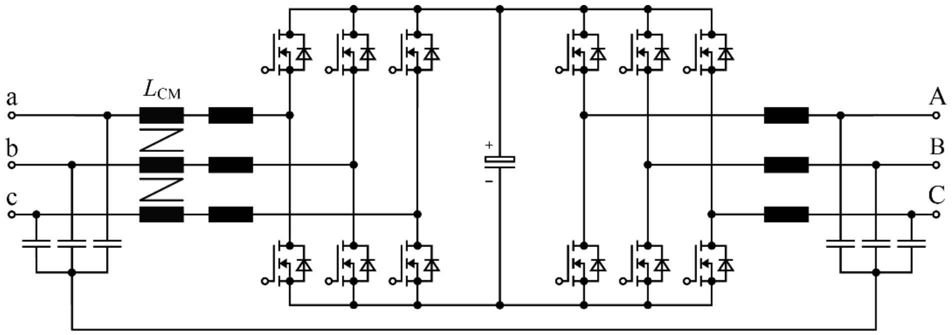

- Higher no. of magnetic components

Comparative Evaluation of VSC/CSC AC-AC Motor Drives

- AC-AC Voltage-Source Converter

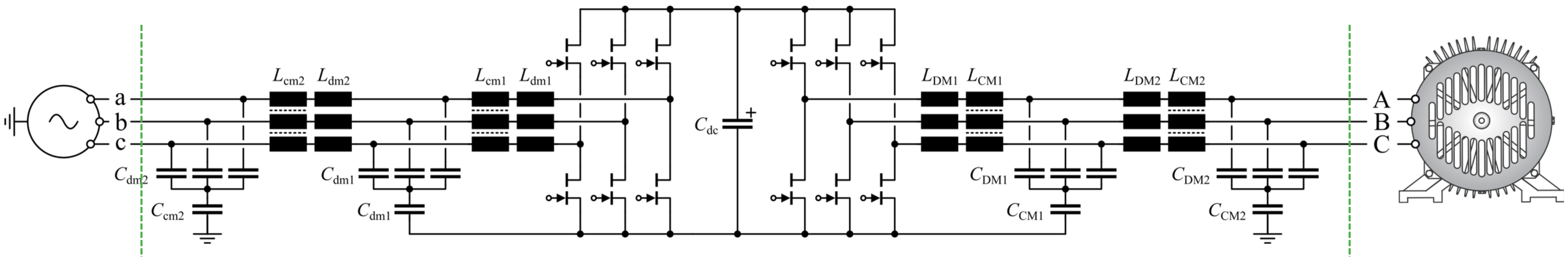

- AC-AC Current-Source Converter

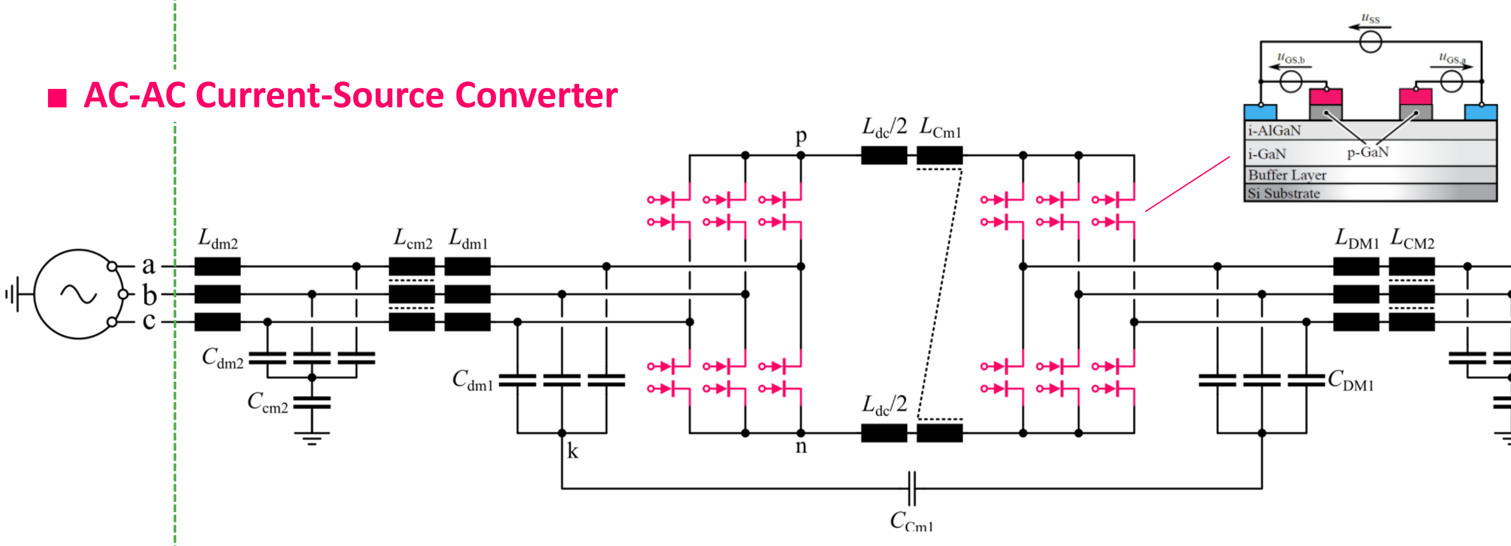

Monolithic Bidirectional 600 V GaN Transistors

Same **EMC Requirements** at grid and motor interfaces
(operation with unshielded motor cables)

Remark: Upcoming EMI Limits for 9…150 kHz

- **Extension of CISPR 11 / IEC 61800-3 towards lower frequencies**
- IEC TS 62578 (2015): recommendations for active infeed converters

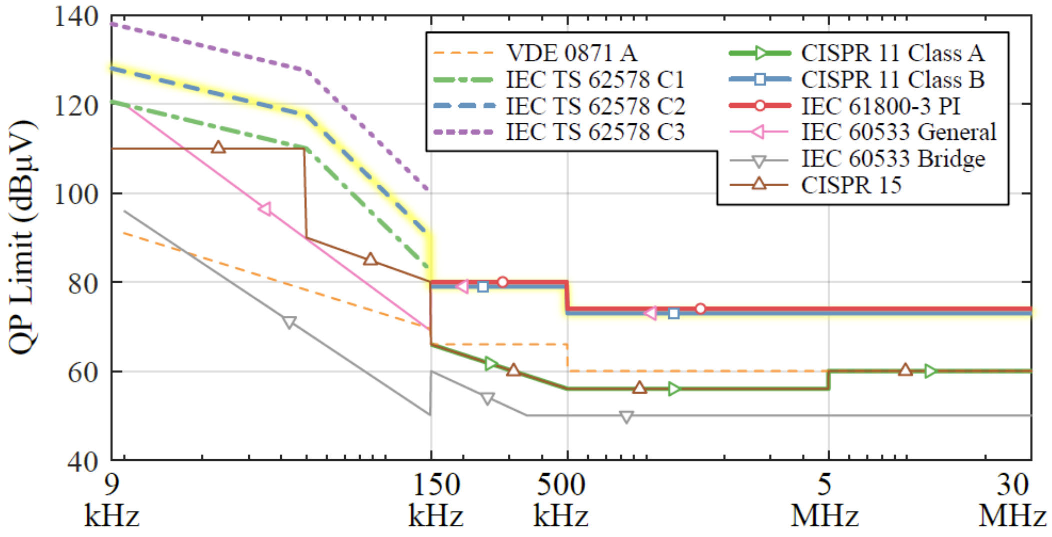

Exemplary unfiltered noise emissions (simulation)

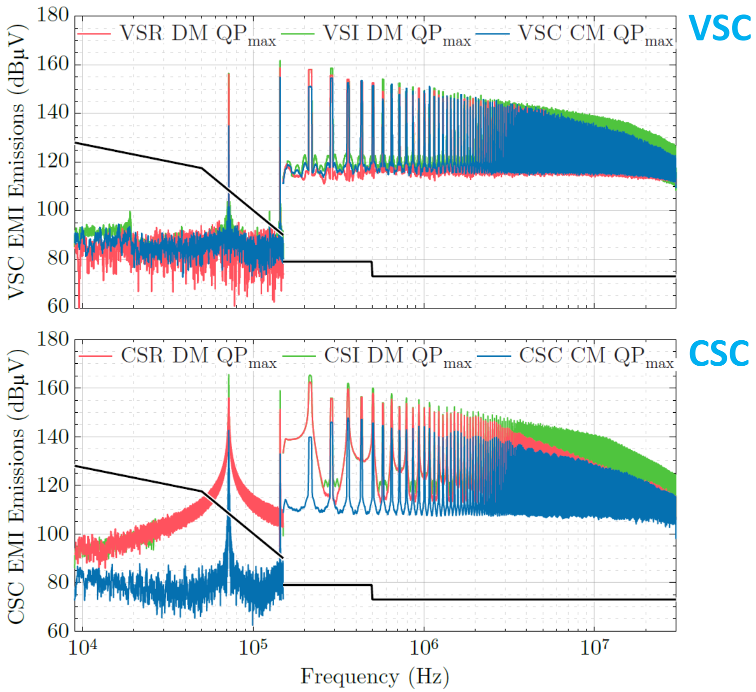

- Next-generation, future-proof designs | Proactively consider upcoming rules | **Full EMC in 9 kHz…30 MHz**

Comparative Evaluation of VSC/CSC AC-AC Motor Drives

■ Semiconductor Efficiency

$\eta_{sc} = 1 - P_{loss,sc} / P$

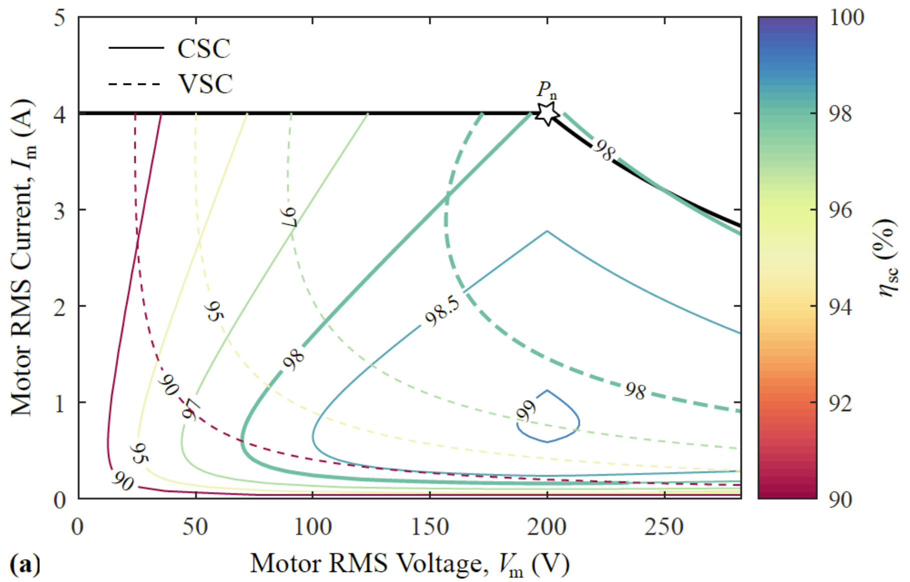

■ Relative Semiconductor Losses

$p_{loss,sc} = P_{loss,sc} / P_{nom}$

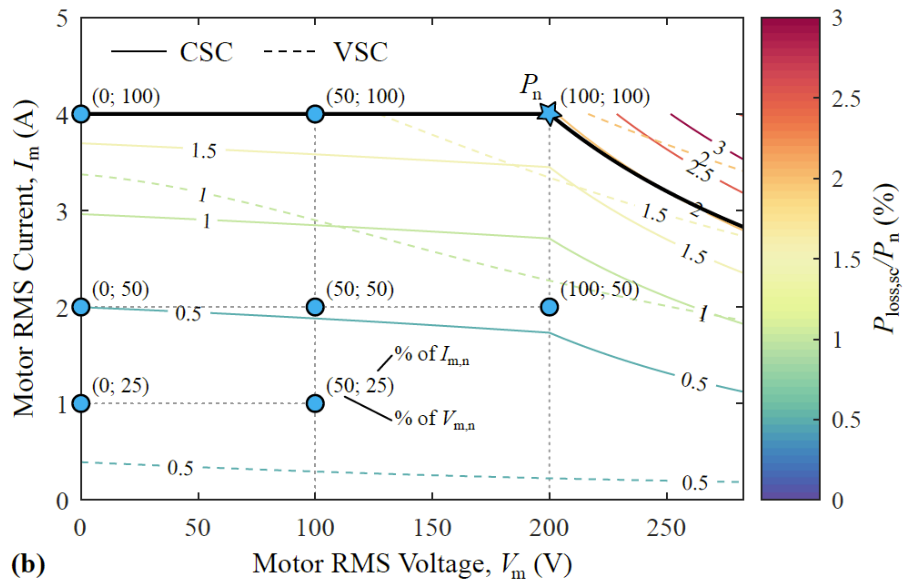

● Representative OPs defined in EN 50 598

Ecodesign for drive systems

- 200 V grid voltage | 4 A nominal motor RMS current | 72 kHz switching frequency
- Roughly equal chip area for VSC and CSC | Similar performance at nominal OP | Same EMI behavior
- **Outlook:** EMI filter comp. modeling | Comparison of volume, weight, control dynamics, … | IPEC 2022 ECCE ASIA

Image: freepik.com

Remark: Self-Reverse-Blocking MBDS – Concept

- **CSI/CSR often operate with unidirectional DC-link current**
  - HV Switch + HV Diode: HV diode characteristic / high cond. losses
  - MBDS: Ohmic cond. char. but 2 external gate signals / 2 gate drives
  - "Self-Switching": Ohmic cond. char. but high local complexity (sensing)
- **SRB-MBDS: Quasi-ohmic cond. char. (cascode with LV Si Schottky diode) and 1 external gate**

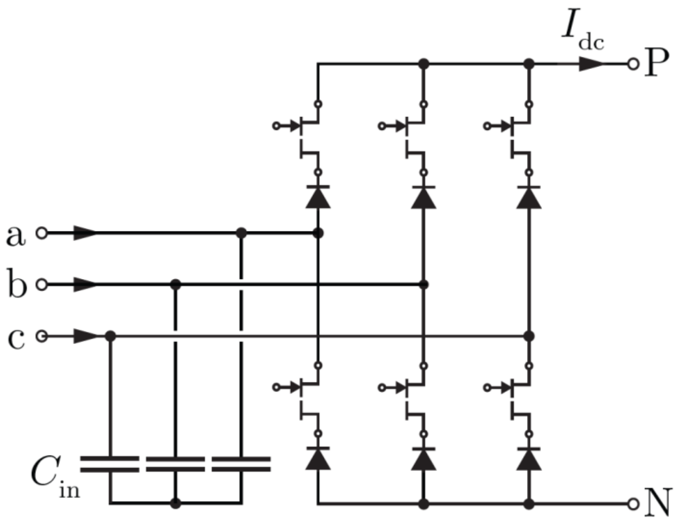

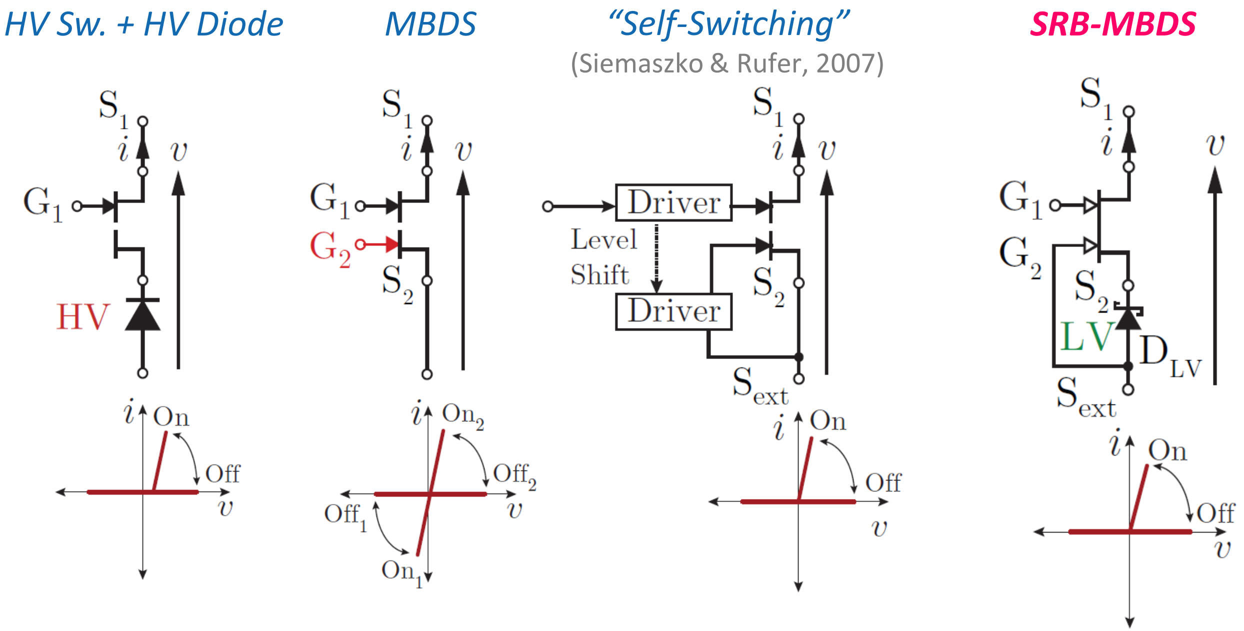

Remark: Self-Reverse-Blocking MBDS – Verification

- **Proof-of-concept exp. verification with discrete components**
  - 190 mΩ, 600 V GaN MBDS and 40 A, 10 A Si Schottky diode

- **Integration / co-packaging of MBDS and LV diode for improved performance**

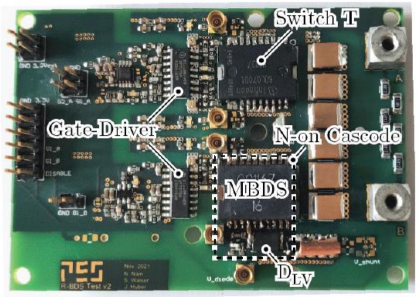

Conduction characteristics

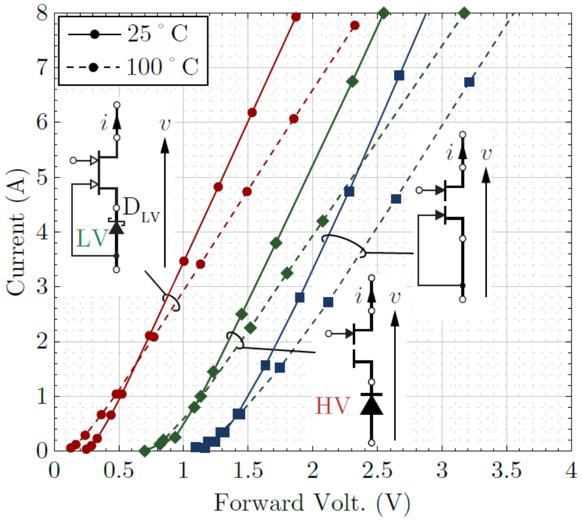

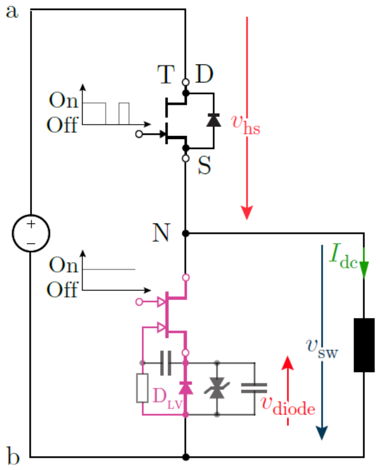

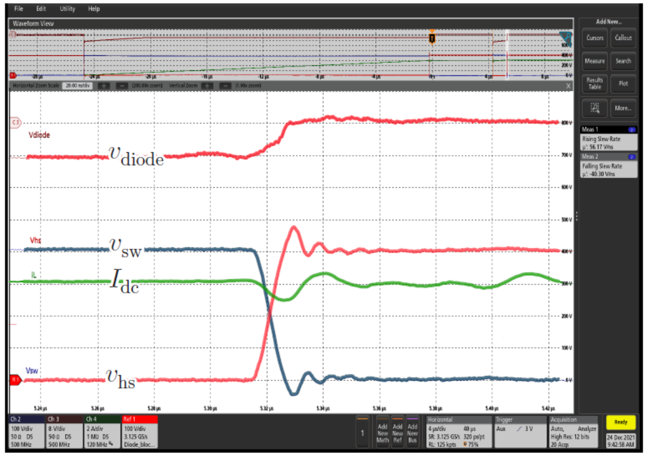

SRB-MBDS turn-on (diode)

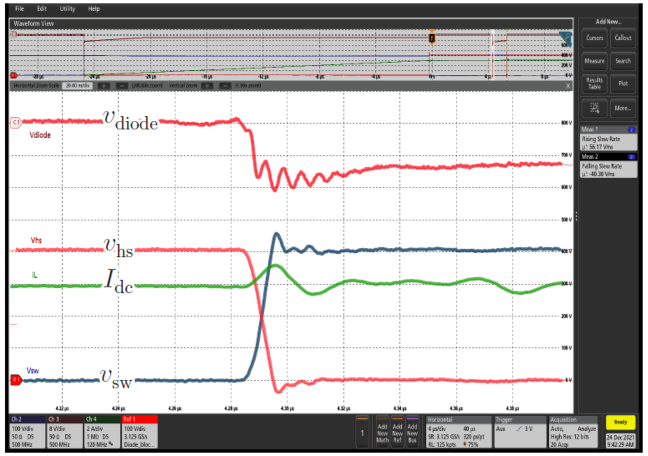

SRB-MBDS turn-off (diode)

Details in upcoming TPEL letter!

Conclusion & Outlook

Conclusion

- **Novel 600 V, 140 mΩ *true* monolithic bidirectional GaN switches from** infineon
  - Removes structural disadvantages of current-source topologies
  - Interesting for 800 V DC-link 3-Level T-Type voltage-source topologies

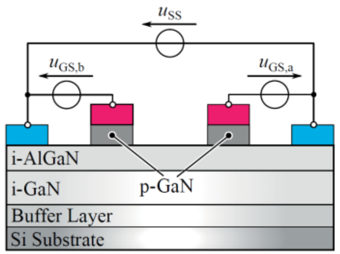

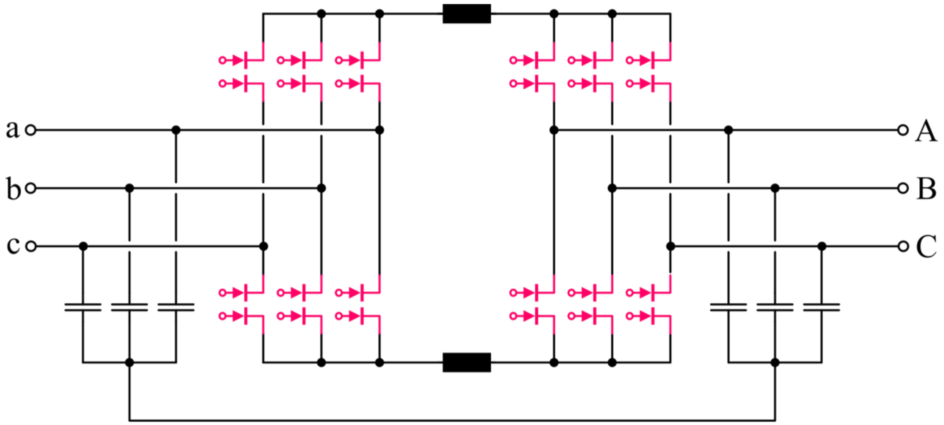

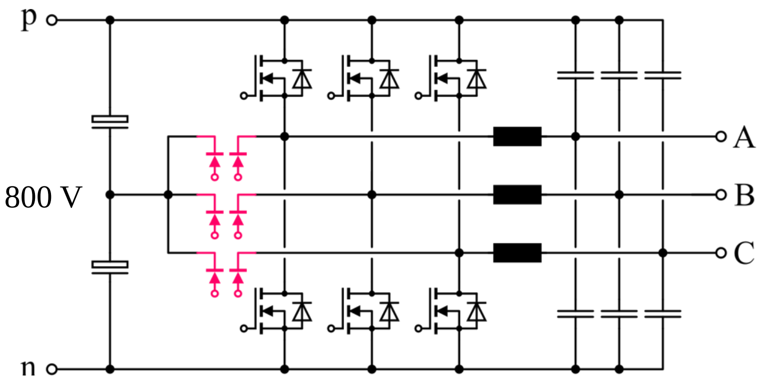

- **Next-generation motor drives: AC-AC Current-Source Converters vs. AC-AC Voltage-Source Converters**
- **Availability of *true* MBDSs shifts trade-offs | Full comparative re-evaluation required/ongoing**
- **GaN M-BDS technology takes flight and promises straightforward designs and superior performance**

Thank You!

Slide download

http://u.ethz.ch/8c7bF